METEOR-Berichte

Benthic element cycling, fluxes and transport of nutrients and trace metals across the benthic boundary layer in the Peruvian oxygen minimum zone (SFB 754).

Cruise No. 137

06.05. – 29.05.2017
Callao (Peru) – Callao

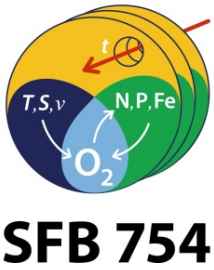

Stefan Sommer, Marcus Dengler
and shipboard party
Chief Scientist Stefan Sommer
GEOMAR Helmholtz Centre for Ocean Research Kiel

2019

Table of Contents

1 Summary

The magnitude of nutrient and trace metal release from oxygen minimum zone (OMZ) sediments as well as their fate in the water column is of utmost importance for the pelagic nutrient budget and consequently for the ongoing expansion of OMZs. The major aim of this research cruise that was conducted within the framework of the Kiel collaborative research center SFB 754 (Climate – Biogeochemistry Interactions in the Tropical Ocean), was to study the effects of variable environmental conditions on benthic element turnover and exchange with the bottom water under natural conditions of austral fall/winter but also during experiments. This allows the quantitative simulation of benthic-pelagic nutrient- and trace metal budgets over longer time periods. The experimental investigations aimed to specifically resolve the contribution of sulfur bacteria and denitrifying foraminifera controlling benthic N, P and S fluxes. The investigation of mixing processes in the bottom boundary layer (BBL) and quantification of diapycnal and advective fluxes across the BBL and the stratified water column will be used to resolve the fate of these substances.

The multidisciplinary study mainly focused on a depth transect at 12°S and is scientifically closely linked to the METEOR cruises M135, M136 and M138. In order to achieve the scientific goals an intense physical, biogeochemical and biological working program was conducted in the water column and at the seafloor accompanied by shipboard experiments. Studies in the water column comprised 92 CTD, 65 microstructure CTD, 18 TM-CTD and 14 in situ pump deployments. Sediment samples were obtained during 47 mulitple-corer and 12 Lander deployments. Additionally, lander deployments were performed to obtain time series of physical parameters and the current regime in water depths of 76 and 128m. The deployment of these instruments covered the time period of cruises M136 and M137.

We slightly deviated from the cruise proposal and spent a minor amount of the station time along a zonal transect at 12.3°S in order study the biogeochemistry during eddy formation. Eddy formation cannot be predicted and hence planned in a cruise proposal, however their study bears a high scientific potential and is a central part of the SFB745 research activities. Due to the good weather conditions all deployments were successful, hence all the data and sample material aimed for has been achieved. It is to expect that as planned all scientific questions can be addressed. Especially, the joined synthesis including the data of the other recent SFB cruises M135, M136 und M138 and their comparison with the earlier SFB-cruises M77, M92 harbor a high scientific potential.

Zusammenfassung

Die Stärke der Rückführung von Nährstoffen und Spurenmetallen aus Sedimenten innerhalb der Sauerstoffminimumzonen (SMZ) als auch deren Verbleib ist für den pelagischen Nährstoffhaushalt und damit für die gegenwärtig beobachtete Ausbreitung von Sauerstoffminimumzonen (SMZ) von entscheidender Bedeutung. Zielsetzung dieser Reise, die im Rahmen des Kieler SFB754 (Climate – Biogeochemistry Interactions in the Tropical Ocean) durchgeführt wurde, war es die Auswirkungen variabler Umweltbedingungen auf den Stoffumsatz und -austausch der Sedimente mit dem bodennahen Wasserkörper sowohl vor dem natürlichen Hintergrund des beginnenden Südwinters als auch experimentell zu erfassen. Dies ermöglicht die modellhafte Quantifizierung des benthisch-pelagischen Nährstoff/ Spurenmetallbudgets auch über längere Zeiträume. Im Vordergrund der experimentellen Untersuchungen stand die Frage zu welchem Ausmaß die benthischen N, P und S Flüsse durch Schwefelbakterien und denitrifizierende Foraminiferen kontrolliert wird. Die Erfassung von Vermischungsprozessen in der Bodengrenzschicht und die Quantifizierung von diapyknischen Flüssen zwischen bzw. entlang der Bodengrenzschicht und der geschichteten Wassersäule soll Auskunft zum Verbleib dieser Stoffe geben.

Die multidisziplinären Arbeiten fanden vorwiegend entlang eines Tiefenschnitts bei 12°S statt und sind wissenschaftlich sehr eng mit den METEOR Reisen M135, M136 und M138 verknüpft. Um diese Zielsetzungen zu erreichen, wurde ein umfangreiches physikalisches, biogeochemisches und biologisches Messprogramm sowohl in der Wassersäule als auch am Meeresboden durchgeführt. Das Arbeitsprogramm in der Wassersäule umfasste insgesamt 92 CTD, 65 Mikrostruktur CTD, 18 TM-CTD und 14 in situ Pumpen-Einsätze. Sedimentproben wurden mittels 47 Multicorer-, und 12 Lander Einsätzen erhalten. Zusätzlich wurden Lander-Einsätze zur Zeitserien Erfassung von physikalischen Parametern und der Strömung bei Wassertiefen von 76 und 128 m durchgeführt. Diese Instrumente kamen für die Dauer der Reisen M136 und M137 zum Einsatz.
Abweichend vom Fahrtantrag wurde im geringem Umfang Stationszeit entlang eines zonalen Schnitts bei 12.3°S verbracht um die Biogeochemie bei der Eddy-Bildung zu erfassen. Solche Ereignisse lassen sich nicht vorhersehen, bergen jedoch ein hohes wissenschaftliches Potential in sich und sind zentraler Bestandteil der SFB754 Forschungsaktivitäten. Die Einsätze verliefen auch aufgrund der guten Wetterbedingungen hervorragend, somit steht das angestrebte Datenmaterial zur Verfügung. Es ist zu erwarten. dass die wissenschaftlichen Fragestellungen zu einem breiten Umfang adressiert werden kann. Hierbei liegt in der Synthese der Datensätze verschiedener Fachdisziplinen sowie die Einbeziehung der anderen SFB Reisen M135, M136 und M138 und der Vergleich mit früheren SFB-Reisen in diese Region (z.B. M77, M92) ein hohes wissenschaftliches Potential.

2 Participants

2.1 Prinicpal Investigators

Name	Institution
Prof. Dr. Achterberg	GEOMAR
Prof. Dr. Dagan, Tal	CAU
Dr. Dale, Andrew W.	GEOMAR
Dr. Dengler, Marcus	GEOMAR
Dr. Gasser, Beat	IAEA
Dr. Glock, Nico	GEOMAR
Dr. Roy, Alexandra-Sophie	CAU
Dr. Sommer, Stefan	GEOMAR
Prof. Dr. Treude Tina	UCLA

2.2 Cruise Participants

Name	Discipline	Institution
Dr. Sommer, Stefan	PI. Lander. Biogeochem.	GEOMAR
Beck, Antje	Lander	GEOMAR
Türk, Matthias	Lander Electronics	GEOMAR
Petersen, Asmus	Mechanics	GEOMAR
Clemens, David	PhD Stud. N-Cycle. Lander	GEOMAR
Braasch, Johanna	Student assistant Lander	GEOMAR
Domeyer, Bettina	Geochemistry	GEOMAR
Schüßler, Gabriele	Geochemistry	GEOMAR
Dr. Dale, Andrew	Geochemistry	GEOMAR
Plaß, Anna	PhD Stud. Fe-Cycle	GEOMAR
Utecht, Christine	Geochemistry	GEOMAR
Meier, Karl	Student assistant Geochemistry	GEOMAR
Paul, Karen Mareike	Student assistant Geochemistry	GEOMAR
Dr. Dengler, Marcus	Physical Oceanography	GEOMAR
Müller, Mario	Physical Oceanography	GEOMAR
Lüdke, Jan	Physical Oceanography	GEOMAR
Dr. Thomsen, Sören	Physical Oceanography	GEOMAR
Prof. Dr. Dagan, Tal	Foraminifera	CAU
Dr. Roy, Alexandra-Sophie	Foraminifera	CAU
Dr. Weißenbach, Julia	Foraminifera	CAU
Wein, Tanita	PhD Stud. Foraminifera	CAU
Dr. Glock, Nico	Foraminifera	CAU
Prof. Dr. Achterberg, Eric	Trace Metal Geochemistry	GEOMAR

Mutzberg, Andre	Trace Metal Geochemistry	GEOMAR
Prof. Dr. Treude, Tina	Sulfur Cycle	UCLA
Dr. Gasser, Beat	Radiotracer	IAEA
Langer, Simon	Microbiology. Sulfur Bacteria	IOW
Chuquival, Dennis S. R.	Foraminifera	IMARPE
Bernabe, Wilson J. C.	Carbon Cycle	IMARPE
Rohleder, Christian	Bordwetterwarte	DWD

2.3 Participating Institutions

Name	Institution
GEOMAR	Helmholtz Centre for Ocean Research Kiel
CAU	Christian-Albrechts Universität Kiel
IAEA	International Atomic Energy Agency. Monaco
IMARPE	Instituto del Mar Peru Esquina Gamarra y General Valle s/n Chucuito – Calloa
IOW	Leibniz Institute for Baltic Sea Research
UCLA	University of California. Los Angeles
DWD	Deutscher Wetterdienst Geschäftsfeld Seeschifffahrt

2.3 Crew

Rank	Name
Master	Hammacher, Rainer
Chief Officer	Dugge, Heike
1st Officer	NN
2nd Officer	Apetz, Derk Ude
Ship's doctor	Rathnow, Klaus
Chief Engineer	Neumann, Peter
2nd Engineer	Brandt, Björn
2nd Engineer	Heitzer, Ralf
Electrician	Starke, Wolfgang
Chief Electronics Engineer	Willms, Olaf
Electronics Engineer	Hebold, Catharina
System Manager	Bagyura, Bernhard
Fitter	Lange, Gerhard
Motorman	Krüger, Frank
Motorman	Schröder, Manfred
Motorman	Kudraß, Klaus
Bosun	Wolf, Alexander

Ships Mechanics	De Moliner, Ralf
Ships Mechanics	Zeigert, Michael
Ships Mechanics	Durst, Alexander
Ships Mechanics	Bußmann, Piotr
Ships Mechanics	Behlke, Hans-Joachim
Ships Mechanics	Hampel, Ulrich
Ships Mechanics	Drakopoulos, Evgenios
Chief Cook	Wernitz, Peter
2nd Cook	Fröhlich, Mike
Chief Steward	Wege, Andreas
Steward	Jürgens, Monika
Steward	Parlow, Jan
Apprentice	Schweiger, Sophia
Apprentice	Staffeldt, Felix

3 Research Program

3. 1 Aims of the Cruise

The magnitude of nutrient and trace metal release from oxygen minimum zone (OMZ) sediments as well as their fate in the water column is of utmost importance for the pelagic nutrient budget and consequently for the ongoing expansion of OMZs. The major aims and questions addressed during the Meteor cruise M137, which was conducted within the framework of the Kiel collaborative research center SFB 754 (Climate – Biogeochemistry Interactions in the Tropical Ocean), were the following:

a. To experimentally elucidate the magnitude and pathways of benthic nutrient fluxes (N, P, Fe other trace metals) in response to enhanced availability of NO_3^- and O_2. The results will be linked to time series of O_2, NO_3^- and NO_2^- in order to allow for better up-scaling and predictive capability of benthic-pelagic coupling in the Peruvian OMZ at seasonal, intra-seasonal, and inter-annual time scales as well as during OMZ expansion.
b. To what extent are benthic N, P and S-fluxes coupled and controlled by filamentous sulfide oxidizing bacteria *Beggiatoa* and *Thioploca* as well as by denitrifying foraminifera? This involves the determination of the turnover of the internal NO_3^-/NO_2^- pools in foraminifera and filamentous sulfur bacteria in response to changing bottom water levels of electron acceptors. It will be determined to what extent foraminifera and sulfur bacteria compete for NO_3^- and NO_2^- resulting into the prevalence of fixed N loss versus recycling. It further encompasses genetic studies of foraminifera as well as studies about the phosphate pools in sulfur bacteria and foraminifera.
c. Another important aspect of the ex situ and in situ experiment series was to determine the timing and magnitude of sulfidic events after stepwise depletion of O_2, NO_3^- and NO_2^- in the bottom water. These studies encompass the determination of the capacity of bacteria and foraminifera to survive conditions of bottom water depleted in O_2, NO_3^- and NO_2^-.
d. To quantify benthic and pelagic cycling of nutrients and trace metals in the OMZ by budgeting physical fluxes of solutes including turbulent fluxes, lateral-diffusive fluxes and advective fluxes in the water column will be combined with benthic flux measurements during austral winter. The measurement program focused on quantifying diapycnal solute fluxes due to turbulent mixing in the water column and particularly in the bottom boundary layer. The findings will be compared to the results from the M92 cruise in austral summer to assess the impact of seasonal changes in stratification on the generation of non-linear internal waves. We expect reduced turbulent mixing to occur during the austral winter period, which is likely to reduce availability of nutrients to the benthic communities and thus reduce benthic turnover rates compared to the austral summer period. Observations of the large-scale boundary circulation and water column nutrient and trace metal distributions will allow quantifying of advective nutrient and trace metal fluxes. Due to the changes in wind forcing, the Peruvian Undercurrent significantly weakens during the austral summer period, which is likely to alter nutrient and trace metal distributions in the water column. In turn, this may feed-back on benthic nutrient availability.
e. The water-column measurement program additionally focused on lateral-diffusive fluxes of nutrients and trace metals by mesoscale eddies and their role in the nutrient budget. Eddies may transport nutrients, trace metals as well as significant amounts of particulate organic matter offshore.

3.2 Agenda of the Cruise and description of the work area

The above objectives will be approached by the joint synthesis of data obtained from the following instruments, whose deployments were conducted according to a spatially and temporarily coordinated sampling scheme: in situ benthic fluxes and experiments using two BIGO type Lander (Biogeochemical Observatory), current measurements, microstructure shear and temperature profiles, high vertical resolution water column sampling using a conventional CTD water sampling rosette (CTD), a specific Trace Metal CTD water sampling rosette (TM-CTD) as well as Gliders and a Microstructure CTD (MSS). The water column program was supplemented with in situ Pump deployments (ISP) for radiotracer and microbiological investigations. Time series measurements of currents and physical properties of the water column were conducted using 2 benthic mini-landers (SML and POZ) that were equipped with upward-looking ADCPs. The in situ benthic measurement- and experiment program was supplemented by sediment retrieval using a video controlled Multiple Corer (MUC), which were used for ex situ experiments, geochemical and biological (foraminifera, sulfur bacteria) investigations.

The focus of the investigations was on a depth transect at 12° S (Fig. 3.2.1, 3.2.2). This area was also part of the research program of the previous METEOR cruises M90, M91 and M93 as well as M136. Along this depth transect, stations for the in-situ flux measurements that were started during cruise M136 were completed. They comprise water depths of about 75, 100, 130, 145, 195, 243, 302, 752 and 984 m. Subsequently, lander based in-situ experiments were specifically conducted in water depths of 74, 129, 193 and 302 m, which were densely populated by sulfur bacteria and foraminifera.

In addition to the actual transect at 12°S a small water column program was conducted along a zonal transect at 12.3°S. In this area, we witnessed the formation of an eddy, which is known to strongly affect the water column geochemistry. Hence we used this unique opportunity to perform additional water column investigations.

Overall, we conducted 92 CTD casts, 65 MSS deployments, 18 TM-CTD casts as well as 47 and 12 deployments of the MUC and the BIGO Lander respectively. The working program further included deployments of the Glider, Fish and the Rapid Cast system. The Fish is a device for the continuous sampling of surface water. It was mostly deployed within the stations and treated as one station (M137-615). The Rapid Cast system is a device for repeated measurements of physical properties in the surface layer.

According to the ship time proposal we successfully conducted measurements at all planned stations. We followed the DFG regulations summarized in the „Erklärung zu einer verantwortungsvollen Meeresforschung“ and the (OSPAR) Code „Code of Conduct for Responsible Marine Research in the Deep Seas and High Seas of the OSPAR Maritime Area” to avoid unnecessary environmental and ecosystem disturbances. The impact of the conducted work to the environment was very minor. All lander were recovered. There were no activities, which could lead to substantial physical, chemical, biological or geological changes or damage of marine habitats. Care was taken to avoid activities, which could disturb the experiments and observations of other scientists. We made use of the most environmentally-friendly and appropriate study methods, which are presently available, and avoided collections that are not essential to conduct the scientific research. The number of samples was reduced to the necessary minimum.

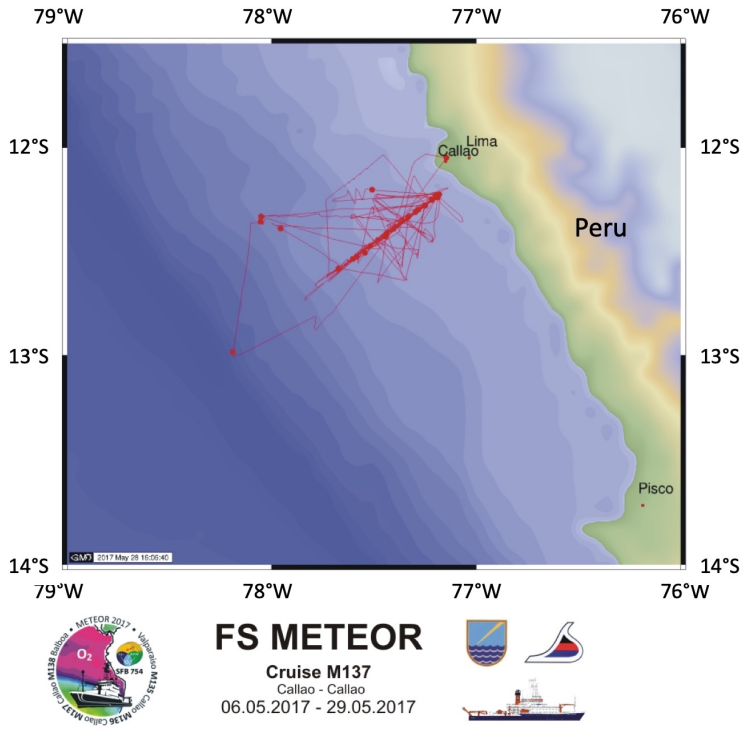

Fig. 3.2.1 Track plot of the cruise M137 off Peru. The cruise started and ended in Callao. Major focus was on a depth transect at 12°S.

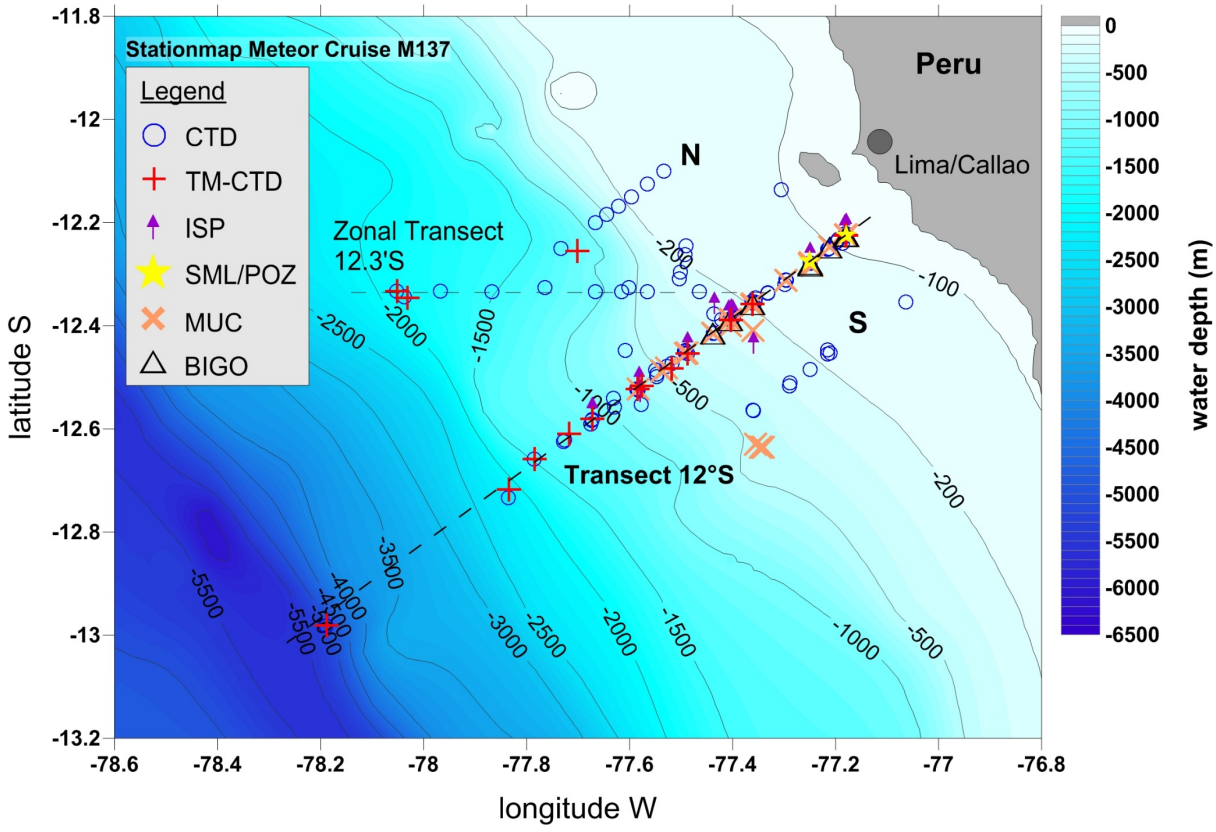

Fig. 3.2.2 Detailed station map of the 12°S working area. The entire depth transect covers water depths of 70 to 5000 m and a horizontal distance of about 45 nm. A short transect at 12.3°S was sampled to investigate the effect of eddy formation of water column geochemistry

4 Narrative of the cruise

At the 4th of May 14 scientists arrived in the evening hours onboard of RV METEOR. Participants from IMARPE (Instituto del Mar del Perú. Peru) and UCLA (US) arrived at the 5th of May, whereas the remaining participants were already on board from the previous cruise M136. The harbour time was used to establish the laboratories or to maintain gears that were used during the previous M136 cruise. At the 4th of May, the German ambassador J. Ranau and collaborators as well as representatives from the Peruvian military visited RV METEOR. We conducted a tour around the ship and introduced the visitors into our scientific gear and research. The visit was very nice and all were very interested. At the following day RV METEOR was visited from pupils of the German-Peruvian School Beata Imelda in Chosica. At the late afternoon, we conducted a small workshop with 11 scientists from IMARPE to discuss first results from the METEOR cruise M136. At Saturday 06th of May at about 09:00 the RV METEOR left Callao during good weather conditions. After a short transit of only about 4 hours, we started with the station work along the depth transect at 12°S. On board was a very diverse team of 29 scientists from 6 different institutions, covering different disciplines including physical-, chemical and biogeochemical oceanography as well as microbiology and ecology, which reflects the interdisciplinary structure of the Kiel collaborative research centre SFB754. Despite the short transit between Callao and the first working station in the working area, the laboratories and scientific gears were ready for deployment allowing to start with the station work. The depth-transect at 12°S includes 10 main stations in water depths of 74 to about 1000 m but extends to almost 6000 m for water column investigations. Due to the formation of an eddy, which was observed during the previous cruises a small zonal transect at 12.3°S encompassing water depths from 200 down to 1200 m was included into the program.

Since the working area was well known from the previous cruises M92 and M136 a pre-site survey was not required and we were able to immediately start with the regular station work. During the day-time we typically deployed the in-situ pumps, the MUC and the two BIGO-type lander for in situ flux measurements and in situ experiments. During natural flux measurements, the exchange of nutrients, oxygen and DIC inside the two benthic chambers, which were mounted into each lander were measured for time periods of about 32 hours. During experiments the flux chambers were manipulated by adding ^{15}N-nitrate solutions to ambient nitrate levels in the bottom water. During one experiment (BIGO-I-6) at about 80 m water depth ^{15}N-nitrate as well as oxygen was added.

Ex situ experiments on board of the RV METEOR investigating the turnover of foraminifera and sulphur bacteria represented a major focus of this research cruise. The single celled eukaryotic foraminifera and the filamentous sulphur bacteria are important for the turnover of nitrogen compounds and with regard to sulphur bacteria also for the phosphorous cycling. Five scientists (CAU, GEOMAR) were specifically dedicated to the investigation of the single celled foraminifera. which in high densities populate the sediment surface of the Peruvian oxygen minimum zone. The investigation of denitrification rates of single species, incubation of the entire sediment system as well as sampling for latter genomic, transcriptonomic and morphological analyses were the focus of these studies. One scientist (IOW) was dedicated to the investigate phosphate turnover in filamentous sulphur bacteria.

At night, we typically deployed the CTD water sample rosette for physical and nutrient measurements, a specifically designed TM-CTD for trace metal measurements and a microstructure CTD for turbulence measurements. We further deployed and took care of the Glider swarm for autonomous and continuous measurements of physical parameters, currents, oxygen as well as nitrate. During all activities, the shipboard ADCP was used for current measurements. During transits the Fish and a Rapid Cast System was deployed. The two small-sized lander SML and POZ were used to continuously record currents and physical parameters during the Meteor cruises M136 and M137 in water depths of 74 and 128 m. The landers were recovered at the 25th

of May. This station work was continued until the end of the cruise. We achieved all planned scientific aims.
During most days, the weather was calm with south-easterly winds in the range of 3 to 4 Bft with a swell of about 2 m allowing for smooth operations of the different gears. Only during mid-May weather conditions changed due to a strong low, which formed off Chile resulting in high swell of 4 m. Towards the end of the cruise wind force was between 5 and 6 Bft and swell was up to 3.5 m. However, these weather conditions didn´t affect station work. Just two days prior to the end of the cruise, we had a problem with the Trace Metal winch and we recommended for the next cruise to solve this problem. At the 28th of May, the gear and scientific instrumentation was packed and all laboratories were cleaned. At the 29th RV METEOR headed to the harbor of Callao and most scientists disembarked for their flights back to Germany. A small group of scientist stayed on board to take care of the container shipping.

5 Preliminary Results

5.1. Physical oceanography and biogeochemical water column measurements

5.1.1 Hydrography from CTD and Rapid Cast measurements

(G. Krahmann, M. Dengler, S. Thomsen, J. Lüdke, S. Sommer)

CTD system and calibration:

During M137, a total number of 92 CTD profiles were collected in most cases to full ocean depth. Positions and profiling depth of the casts are detailed in section 7.1. During the whole cruise the GEOMAR SBE7, a Seabird Electronics (SBE) 9plus underwater unit, was used. It was attached to a GO4 rosette frame. The SBE7 was equipped with one Digiquartz pressure sensor (s/n 1162) and double sensor packages for temperature (T), conductivity (C) and oxygen (O2) (primary set: T1 = s/n 4051, C1 = s/n 2512, O1 = s/n 2669; secondary set: T2 = s/n 2120, C2 = s/n 3374, O2 = s/n 992). Additionally, fluorescence and turbidity sensors (Wetlabs) were attached to the SBE7 and a sensor measuring nitrate concentrations. To collect water samples 24 10-liter bottles were attached to the rosette frame. All sensors worked well throughout the cruise. Data acquisition was done using Seabird Seasave software version 7.23.2.
For calibration of the CTD conductivity and oxygen sensors, conductivity values were determined from 154 water samples using a Guildline Autosal salinometer (AS) and oxygen concentrations were determined from 269 water samples using Winkler titration. Throughout the cruise, conductivity values from the water samples were analyzed using the GEOMAR salinometer AS 8 (Model 8400 B). During the 18 days when the instrument was in use, only small adjustments to the standardization potentiometer were necessary and subsequent sub-standards determinations within each day indicated an adequate stability of the instrument. For Winkler titration measurements, the same measurement setup and titration procedures as during M135 and M136 were used. For details, the reader is referred to section 5.2.1 in the M135 cruise report (Visbeck et al., 2018).
CTD conductivity was calibrated using linear dependencies of pressure, temperature and conductivity to match the salinometer derived values. CTD oxygen was calibrated using linear dependencies of pressure, temperature and oxygen as well as 2nd order in oxygen and the product of oxygen and pressure. The misfit, taken here as the root-mean square (rms) of the differences between CTD values and the respective water samples, was 0.00010 S/m and 0.00010 S/m for the C1 and C2 sensors, respectively. The conductivity misfit translates into a salinity misfit of 0.0010

psu and 0.0010 psu. The misfits for O1 and O2 sensors on M137 were 0.39 and 0.38 µmol/kg, respectively. For each fit, the 33% most deviating water samples values were removed to exclude biases by bad samples. For the final data set that will also be publicly available, the primary sensor set was used for all CTD stations. Data from the fluorescence and turbidity sensors and the PAR sensor were calibrated by the calibration coefficients provided by the manufacturer. No further corrections were applied. Data from Nitrate sensor (type SUNA, manufactured by Seabird Satlantic, s/n 761) were calibrated against 1149 Nitrate measurements made from water samples. The independently collected and processed nitrate data was later merged with the CTD data.

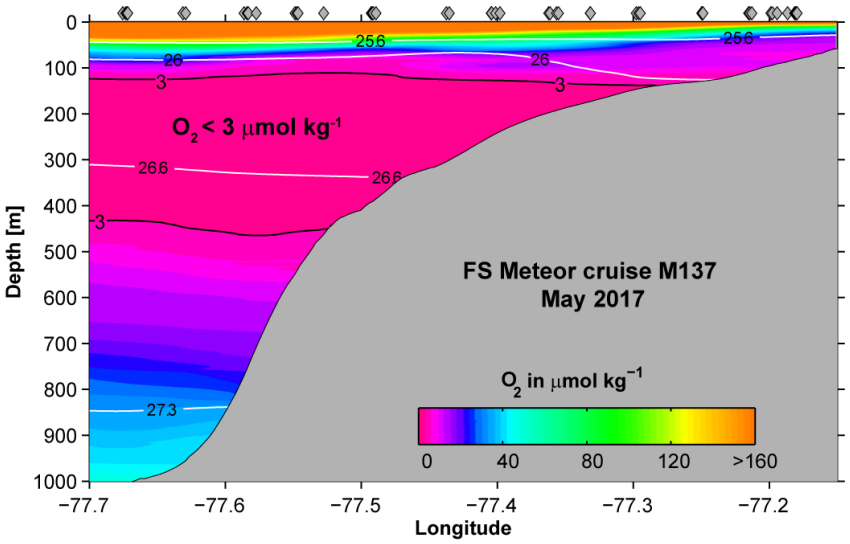

Fig. 5.1.1.1: Longitude-depth distribution of dissolved oxygen concentration along the transect 12°S. Diamonds above the plot indicate positions of CTD stations. White contours indicate isopycnals (σ_θ) in kg m^{-3}. The thick black solid line shows represents an oxygen concentration of 3 µmol kg^{-1}.

CTD system preliminary results:

In the upper ocean along the 12°S transect, we encountered anomalous warmer, saline, and oxygenated waters compared to previous cruises. In the upper 80m, waters were between 1°C-2°C warmer and between 0.02psu and 0.03psu richer in salinity. We presume that this water was associated to the coastal El Niño event that had occurred in northern Peru just two month prior to the cruise. The coastal El Niño event was connected to heavy and devastating rainfalls favored widespread land sliding and extensive flooding in large parts of Peru.

This anomalous water mass was also rich in oxygen leading to well oxygenated waters on the shelf and across the 12°S transect in depth shallower than 100m (Fig. 5.1.1.1). During previous cruises, waters below 30m depth on shelf and below 60m offshore of 77.4°W were anoxic. A first analysis suggests that the anomalous water mass likely originated from above the EUC core at the equator and was rapidly advected southward along the continental margin off Peru.

Rapid Cast:

A total of 743 underway conductivity-temperature-depth (uCTD) profiles were collected during the cruise using an automated Teledyne Rapidcast system. Two (s/n 54 and 155) probes measuring and internally recording pressure, temperature and conductivity were used throughout the cruise. For the calibration of the sensors the probes were attached to the CTD rosette to identify possible pressure offsets, which were found to be very small. The subsequent calibration of temperature and salinity included a thermal lag correction and a comparison between the CTD-calibrated thermosalinograph and the uCTD measurements. All measurements of the uCTD probes agreed well with the thermosalinograph values. In neither probe a drift was found throughout the cruise.

5.1.2 Turbulence measurements using microstructure sensors

(M. Dengler, S. Thomsen)

A microstructure measurement program was carried out to quantify pelagic diapycnal fluxes of oxygen, nutrients and other solutes along the Peruvian continental slope and shelf. Additionally, the program aimed at advancing the understanding of the mixing processes at the continental slope and shelf. Here, tide-topography interaction generates baroclinic tides and nonlinear internal waves (e.g. Mosch et al., 2012; Erdem et al., 2016) that lead to enhanced near-bottom and near surface mixing.

The measurement program consisted of autonomous turbulence sampling by two gliders equipped with microstructure sensors (see section 5.1.4) and of shipboard microstructure sampling using a profiling system manufactured by Sea & Sun Technology. For the ship-based microstructure measurements a MSS90-D profiler (S/N 73), a winch and a data interface was used. The loosely-tethered profiler was optimized to sink at a rate of 0.55 ms^{-1}. In total, 258 profiles were collected during 65 microstructure stations. The profilers were equipped with three shear sensors, a fast-response temperature sensor and oxygen sensor, an acceleration sensor, two tilt sensors and conductivity, temperature, depth sensors sampling with a lower response time. A comparison with the CTD oxygen sensor data showed that the oxygen sensor of the microstructure probe, a fast optical sensor with a response time of about 2 seconds, was able to resolve vertical small-scale variability of oxygen. The O_2 sensor on the profiler thus proved to be adequate to resolve the elevated oxygen gradients in the water column. During the whole cruise, shear sensor sn 134 was attached to channel S1, shear senor sn 135 was attached to S2 and shear sensor sn 125 was attached to S3. The shear sensors and all other sensors worked well throughout the cruise.

5.1.3 Vessel-mounted current measurements

(J. Lüdke, M. Dengler)

Technical aspects:

Upper-ocean velocities along the cruise track were recorded continuously by the two vessel mounted ADCP systems of R/V METEOR. The 38 kHz RDI Ocean Surveyor (OS38) system was operated in narrowband mode with 32 m bins and a blanking distance of 16 m while 55 bins were recorded. The 75 kHz RDI Ocean Surveyor (OS75) was operated in narrowband mode recording 100 bins of 8 m length and a blanking distance of 4 m as on the previous cruise until May 11. From then onward, the setup was modified to record 55 bins having a bin length of 16m to improve the signal to noise ratio due to low density of backscatters in the OMZ depth range. The measurement range of the OS75 was about 800 m. The OS38 recorded valuable data to about 1200 m depth during the whole cruise.

Data post-processing carried out for both systems included water track calibration of the misalignment angle and the amplitude of the Ocean Surveyor signal (Tab. 5.1.3.1). Processing and calibration where performed together with the previous cruise M136 for OS38 and for OS75 for the time when 8m bins were recorded. Calibration of the OS75 for the time periods recording 8 m bins and 16 m bins resulted in very similar values. The difference is smaller than the standard deviation and statistically insignificant.

Tab. 5.1.3.1 Misalignment angles and amplitude of the different Ocean Surveyors.

OS	Mode	Bin length	Misalignment angle ± Standard deviation	Amplitude factor ± Standard deviation
75	NB	8 m	-1.0267 ± 0.65097	1.0054 ± 0.013144
75	NB	16 m	-1.0267 ± 0.59584	1.004 ± 0.01003
38	NB	32 m	-0.43998 ± 0.74786	1.0037 ± 0.01519

Preliminary results:

The alongshore flow in the Peruvian upwelling region is dominated by the poleward flowing Peru-Chile Undercurrent (PCUC). At 11°S, the PCUC usually occupies the depth range between 20m and 400m depths and exhibits maximum average flow speeds of about 0.1 ms^{-1} between 50 and 100m depths (e.g. Chaigneau et al, 2013). During M137 however, poleward alongshore flow intensified until mid-May, when velocities above 0.6 ms^{-1} were recorded in the PCUC core (Fig. 5.1.3.1). Furthermore, the PCUC velocities exceeded those observed during the previous cruise M136 by more than a factor 3. This current intensification was most likely caused by the passage of an intra-seasonal coastally trapped wave as described previously by Pietri et al (2014).

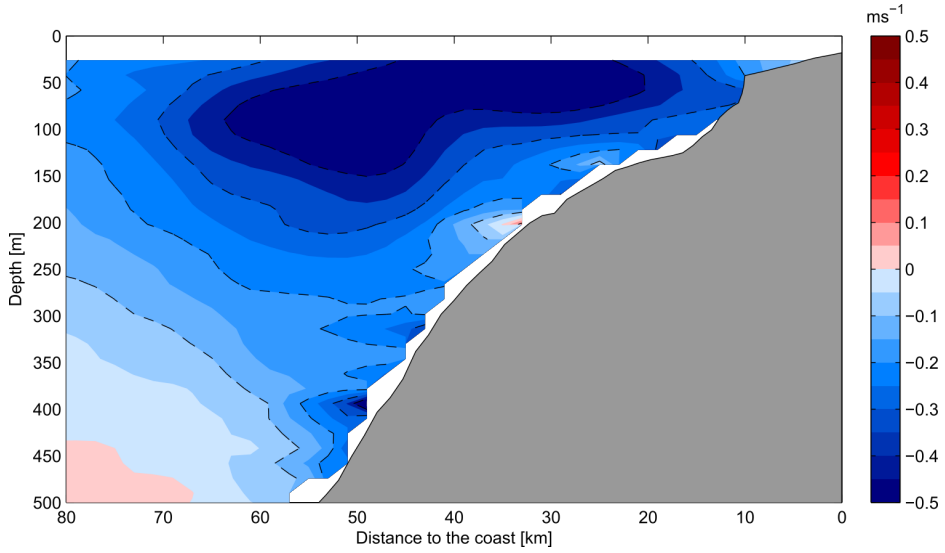

Fig. 5.1.3.1: Alongshore velocity at 11°S measured by the 75 kHz vessel-mounted Ocean Surveyor between May 12 and May 28. Negative values indicate poleward flow.

5.1.4 Glider and oceanographic lander operations

(M. Dengler, G. Krahmann, S. Sommer)

Glider missions:

An integral component of the measurement program of M136 and M137 was the use of autonomous measuring platforms (ocean gliders) to measure hydrography, turbulence, and various biogeochemical parameters at high spatial resolution across the continental slope. Altogether, five Slocum gliders (ifm03, ifm07, ifm09, ifm12, ifm13) were used during eight glider deployments (Fig. 5.1.4.1). The measurement program started with the deployment of two gliders (ifm12 and ifm09) during R/V Meteor cruise M135 on April 3, 2017 and was completed after the recovery of ifm09 (3rd mission) during R/V Meteor cruise M138 on June 11, 2017.

All gliders were equipped with temperature, conductivity, pressure, chlorophyll (chl-*a*), turbidity and oxygen sensors. Apart from the sensors built into the gliders, four of the five gliders carried self-contained sensor packages mounted to the gliders' top. Ifm03 and ifm09 were equipped with a microstructure probe (MicroRider, Rockland Scientific) with two microstructure shear and two microstructure temperature sensors as well as fast-responding accelerometers while ifm12 and ifm13 was equipped with an optical nitrate sensor (SUNA, Satlantic). All internal and external sensors of the gliders worked well throughout the missions.

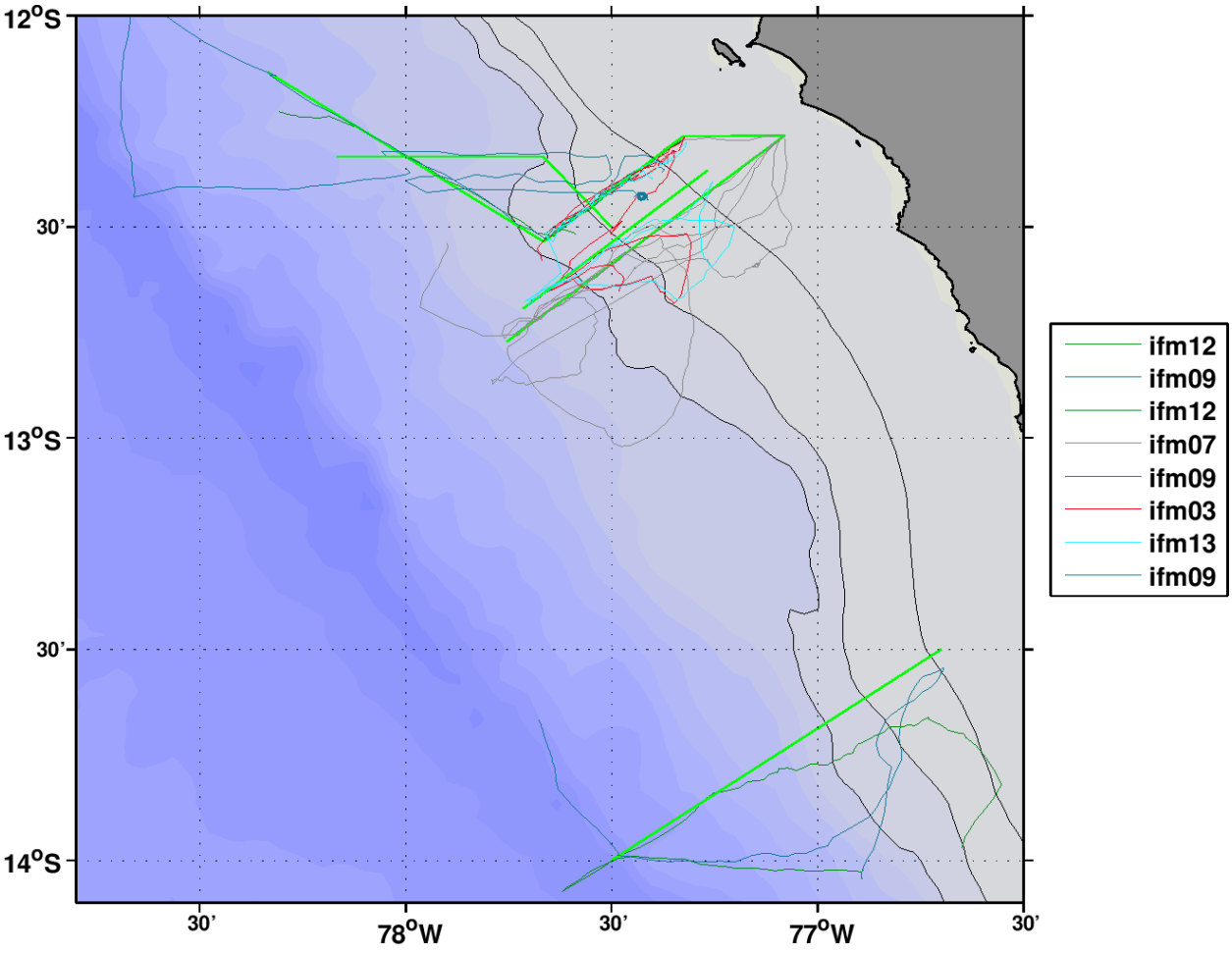

Fig. 5.1.4.1: Tracks of the eight glider missions carried out during the glider measurement program.

During M137, 5 glider operations were carried out. On May 8, glider ifm09 carrying a microstructure package was successfully recovered. The batteries of that glider were replaced and the glider was redeployed on May 26. Three days before, on May 23, glider ifm03 was recovered but not redeployed. Shortly before the end of the cruise on May 28, glider ifm13 was recovered. Finally, on the same day, glider ifm07 was cleaned while in the water. During the cleaning, goose barnacles and seaweed that had slowed down the glider were removed.

Moorings, oceanographic lander:

A mooring program carried out during M136 and M137 to investigate the variability of the circulation along the continental slope off Peru and to capture internal tides and non-linear internal waves propagating onto the continental slope and shelf. Altogether, four moorings and two oceanographic lander were deployed at different depth along the continental slope near the 12°S

transect. During M137, the two oceanographic landers deployed during the previous cruise were recovered (Tab**. 5.1.4.1)**. The landers were equipped with a RDI Workhorse Sentinel 300 kHz acoustic Doppler current profiler, RBR CTD recorder, a high precision pressure sensor (accuracy of 0.015%), and an oxygen optode. All sensors worked well and delivered excellent data sets.

Tab. 5.1.4.1: Landers recovered during M137.

Mooring	Date and Time (UTC)		Deployment Position[1]		Water Depth
	deployed	recovered	Latitude	Longitude	
Mini Lander SML	24.04. 14:47	25.05. 14:12	12° 13.520'S	077° 10.790'W	75 m
Mini Lander POZ	24.04. 16:43	25.05. 18:04	12° 16.690'S	077° 14.992'W	127 m

5.1.5 Water column nutrient and oxygen geochemistry

(S. Sommer, M. Dengler, J. Lüdke, B. Domeyer, C. Utecht)

Benthic flux measurements that were conducted during the RV METEOR cruises M77(2008), M92 (2013) and the previous cruise M136(2017) along the latitudinal depth transect at 11°S and 12°S showed that particularly at the shelf and upper slope high amounts of ammonium (NH_4^+), dissolved phosphate (PO_4^{3-}), dissolved silica and iron (Fe^{2+}) are released into the bottom water (Bohlen et al. 2011, Lomnitz et al. 2016, Noffke et al. 2012, Sommer et al. 2016). To date the fluxes of solutes from the sediment to the stratified water column and their contribution to the total solute budget of the oxygen minimum zone are poorly quantified. In addition, transport across the shelf and slope is also hardly determined. Coastal upwelling (e.g. Brink 1983) is considered as major transport mechanism to supply nutrients to the mixed surface layer where they contribute to sustain high primary productivity. Near continental boundaries turbulent mixing provides another mechanism that transports nutrients and other solutes to the sea surface and entrain them into the surface mixed layer. In fact, several studies suggest that a significant proportion of the biological production in the surface water is driven by turbulent fluxes of nutrients (e.g. Hales et al. 2009, Rippeth et al. 2009, Schaffstall et al. 2010). The combination of microstructure data (see Section 5.1.2) in combination with nutrient profiles allows to calculate diapycnal fluxes of nutrients and to relate them to benthic fluxes (see Section 5.2.2, and report for METEOR cruise M136).

During the cruise nitrate (NO_3^-), nitrite (NO_2^-), PO_4^{3-} and dissolved silica were measured on-board using an QuAAtro autoanalyzer (Seal Analytical) with a precision of ±0.1 µmol L^{-1}, ±0.1 µmol L^{-1}, ±0.2 µmol L^{-1}, and ±0.24 µmol L^{-1} respectively. Ammonium was measured using the autoanalyzer in addition to the OPA method. A total of 92 CTD water sampling rosette casts were conducted predominantly focusing on the 12°S transect. 78 deployments of which were used for measurements of oxygen in combination with nutrients indicated with “nutrients” in the station list, Chapter 7.

The distributions of oxygen, NO_3^-, NO_2^-, NH_4^+ and PO_4^{3-}in the water column are shown in figure 5.1.5.1. Beside advective transport, the availability of NO_3^- and NO_2^- is strongly related to anammox and denitrification in the water column and in the sediments (see section 5.2.2), which results in the loss of reactive nitrogen from the ecosystem releasing dinitrogen (N_2) into the environment. Under oxygen deficient bottom water conditions at the shelf and the upper slope where the sediments are covered with sulphur bacteria a certain proportion of NO_3^-/NO_2^- might be used for the dissimilatory nitrate reduction to ammonium pathway (DNRA) (e.g. Bohlen et al.

2011, Sommer et al. 2016). During DNRA NO_3^-/NO_2^- is recycled into NH_4^+. Hence reactive nitrogen is retained in the ecosystem opposing the "self-cleaning" effect of denitrification and anammox. DNRA and NH_4^--liberation during ammonification are the main sources sustaining the seabed NH_4^+ release, which eventually fuels water column annamox (Kalvelage et al. 2013). Importantly, another major fraction of NO_3^- and NO_2^- is taken up by foraminifera (protists, Glock et al. 2013, 2019). Beside measurements of seasonal and intra-seasonal variability of water column nutrient distribution, major task of this cruise has been to resolve to what extend NO_3^- and NO_2^- is channeled into foraminiferal denitrification and DNRA facilitated by sulfur bacteria.

Phosphate concentrations were elevated at the shelf and upper slope. This is caused by P release during organic carbon degradation, preferential mineralization of organic P relative to C and reductive iron dissolution (Noffke et al. 2012, Noffke et al. 2016 and references therein). The extent to what transient uptake and release phosphate of sulphurbacteria during shifting bottom water redox scheme is involved still is speculative.

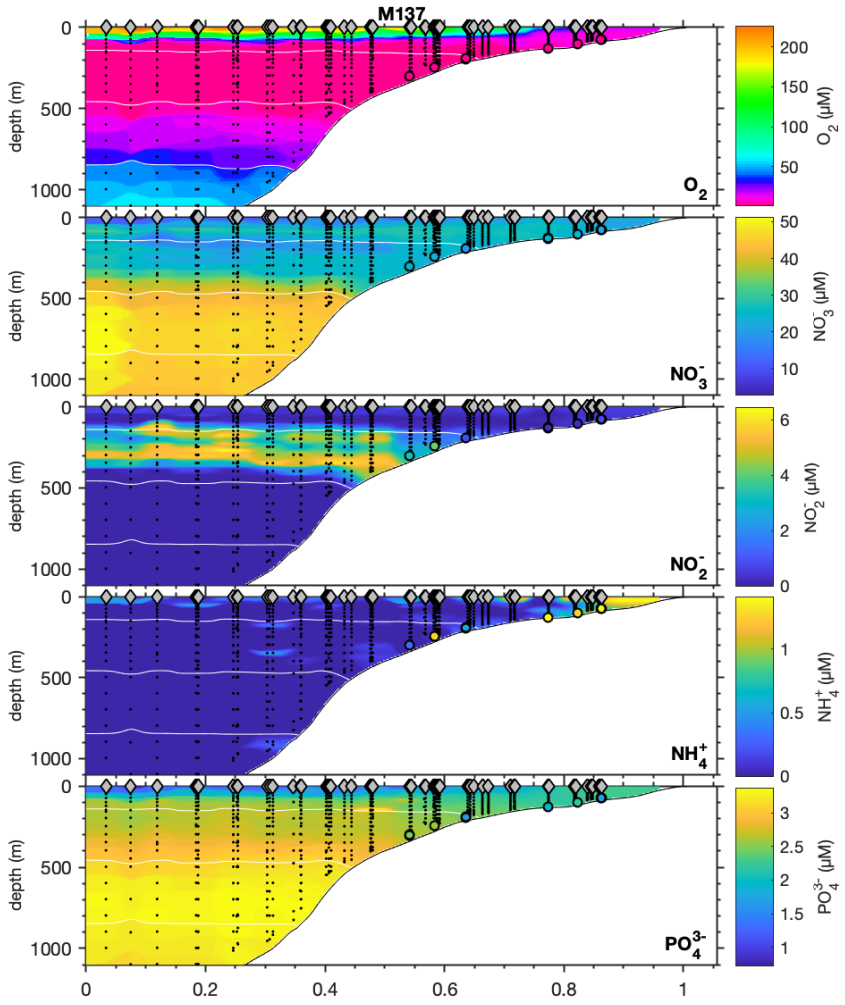

Fig. 5.1.5.1: Distribution of O_2, NO_3^-, NO_2^-, NH_4^+, and PO_4^{3-} along the depth transect at 12°S. The diamonds and black dots indicate the position of the CTD casts and the position of sampling respectively.

5.1.6 Water column trace metal geochemistry

(A. Mutzberg, E. Achterberg)

Trace metal sampling in the water column was planned for 4 RV METEOR cruises M135-M138 with the sampling procedure remaining the same on all 4 cruises. A trace metal clean sampling rosette and winch were operated from METEOR's A-frame with the winch container mounted in the central position at the stern of the ship. A pre-fabricated lab container with in-built air filtration was positioned forward and starboard of this. The trace metal clean sampling rosette was equipped with GO-FLO bottles, which were stored in the trace metal clean lab container when not in use. Prior to the deployment of the trace metal CTD (TM-CTD), GO-Flo bottles were covered with protective plastic caps, bottoms and gloves over the spigots inside the clean container. They were then carried onto deck and mounted onto the trace metal sampling rosette. Immediately (maximum 5 minutes) before deployment the protective plastic was removed. Upon return to deck, gloves were immediately added to the spigots and then the GO-FLO bottles returned to the clean laboratory for sampling.

Sampling for contamination-sensitive parameters (trace metals, particles for elemental analysis, dissolved organic phosphorous (DOP), Fe(II)) was undertaken inside the clean container. Positive air pressure was maintained in the container via a continuous inward air flow, with dust particles in this air flow removed by a HEPA filter. Inside the laboratory, clean suits were worn and all lab-ware was free from exposed metal components. N_2 gas was used to overpressure (0.2 atm) all Go-Flo bottles. O_2 samples were collected immediately after bottles were in the clean container. Sampling then proceeded around the Go-Flo bottles in the order trace metals, DOP/dissolved organic nitrogen (DON), nutrients, salinity.

Overall 17 TM stations were sampled with 222 dissolved trace metal samples collected and acidified for analysis in Kiel.

Trace elements

Samples were collected in acid washed 125 mL LDPE sample bottles for dissolved (0.2 µm filter capsule) trace metal concentrations (metals: Fe, Zn, Mn, Mg, Cu, Co, Cd, Al). Samples were acidified with 180 µL concentrated (10 M) Optima grade hydrochloric acid, in batches and under a laminar flow hood, within 2 days of collection. These samples will be measured on return to GEOMAR via pre-concentration on a SeaFAST system (ESI) and subsequent analysis on an Element 2 ICP-MS (Thermo Scientific) following the method of Rapp et al. (2017). In addition to dissolved samples, 50 samples (10 depths at 5 stations) were re-filtered at 0.02 µm to determine colloidal (0.02-0.2 µm) metals.

Major nutrients and DOP/DON

Samples were collected for dissolved macronutrients (nitrate, nitrite, phosphate, silicate) and dissolved organic phosphate (DOP) and dissolved organic nitrogen (DON) concentration analyses. 20 mL samples were collected in Falcon tubes for macronutrient concentrations. 30 mL samples for DOP analysis were collected separately in acid washed HDPE bottles. DOP/DON samples were then frozen immediately in a -20°C freezer. These samples will be analyzed on return to GEOMAR using a nutrient Auto-analyzer following breakdown of the DOP/DON to inorganic phosphate and nitrate respectively. Macronutrients were stored refrigerated and measured onboard within 1 day of collection (see Section 5.1.5 above).

Particles
For approximately 10 depths at every TM-CTD station, 4 L of seawater was filtered through Sartorius PES 0.2 µm filters to collect sufficient particles for elemental analysis in Kiel. This volume was reduced to 0.5-2 L at coastal stations with high suspended sediment loads. Filters were mounted on plastic, acid cleaned filter holders and attached directly to Go-Flo bottles (still under N_2) and then allowed to drain for approximately 2-3 hours. Filters were then rinsed with de-ionized water (10 mL) and frozen in a -20°C freezer. They will be digested and analyzed via ICP-MS in Kiel.

Underway Tow Fish Measurements (Fish)
Surface (~2-3 m depth) seawater was sampled from a custom-built towed-fish via acid washed 1 cm diameter tubing with suction provided by a peristaltic pump. Water was pumped directly into the purpose-built clean air laboratory container.
16 samples collected during M137 were retained for the determination of dissolved macronutrient concentrations and trace element concentrations. Sample collection for this suite of measurements was carried out with a preference for sampling just before or after (~10-15 minutes) a TM-CTD station. Responsible person for data delivery for trace metals (dissolved and particles) is Mark Hopwood (present affiliation: GEOMAR, e-mail: mhopwood@geomar.de) and for DOP/DON Judith Meyer (present affiliation: GEOMAR, e-mail: jumeyer@geomar.de).

5.1.7 Water column radiotracer and sulfur geochemistry

(B. Gasser, T. Treude)

Both the study on the export of organic matter produced in the euphotic zone and the study on the bacterial sulfate reduction in the water column require the collection of suspended and sedimenting particles sampled from large volumes. We therefore used a set of in situ pumps (McLane Research Laboratories and Challenger Oceanic) in different deployment modes to meet these requirements.

Vertical flux of organic carbon in the water column using radiotracers
(Beat Gasser)
The export of organic matter can be determined by an indirect measurement of the natural radionuclide thorium-234 and its parent radionuclide uranium-238. Thorium-234 shows high reactivity with particles, while it's long lived parent ^{238}U has a conservative behavior and remains soluble in seawater. The "scavenging" of ^{234}Th onto particles produced in the euphotic zone and exported through sedimentation causes a separation between daughter and parent nuclide. The resulting disequilibrium between the two nuclides is used to calculate the flux of particulate organic carbon out of the productive ocean surface layer (Rutgers van der Loeff et al., 2006, Buesseler et al., 2006 and references herein).
During cruise M137, in situ pumps were deployed along the transect at 12°S at water depths of 74, 244, 400, 750 and 1000 m where most of the other sampling devices were deployed, too. See Chapter 7 for the precise position of each in situ pump deployment. Sampling depths were chosen such that the vertical resolution of the resulting profiles represents as well as possible the variabilities in the disequilibrium between the two radionuclides. Productive layers represented e.g. by the chlorophyll maximum were used as indices for those variabilities, and they were identified in the CTD profiles preceding the deployment of the in situ pumps. At each site, two pump casts were done with 4-5 pumps each, except for the site at 74 m depth, where only one

cast with 5 pumps was realized.
Each pump was equipped with 2 filters for particle sampling and 2 cartridges for sampling the dissolved ^{234}Th. One filter (Nitrex tissue) sampled the >70 µm size class considered to represent the settling particles, and the other filter (micro quartz filter of 1 µm nominal size) sampled the suspended particles. Dissolved ^{234}Th was sampled by retention on MnO_2 impregnated cartridges (CUNO Micro-Klean III acrylic), the first cartridge being used for quantifying the ^{234}Th concentration in the water column and the second one for determination of the retention efficiency. On board upon recovery of the in situ pumps, the coarse sized filters were folded, put inside a plastic bag and stored in the freezer (-28°C) and the micro quartz filters were first frozen at -80°C and then stored in the freezer (-28°C) wrapped up in the aluminium paper, in which they had been combusted at 550°C prior to the cruise. For measuring the ^{234}Th activity in the MnO_2 impregnated cartridges they will need to be combusted back at the laboratory, where the ash will be analyzed by gamma spectrometry. The particles from both filters will be analyzed back in the laboratory for their ^{234}Th beta activity. The subsequent measurement of the carbon content on these same particles will be used to determine the C/^{234}Th ratio of settling particles and to calculate the export flux of organic carbon.
Samples for measuring the ^{238}U concentration were obtained from Niskin bottles mounted on a CTD-Rosette. Samples were obtained at the same sites as for ^{234}Th, and the sampling depths were chosen accordingly. Although ^{238}U can be calculated from the salinity, those seawater samples were taken in order to verify the applicability of the calculation in low oxygen waters where redox conditions may alter the solubility of ^{238}U. The measurement of ^{238}U itself will be done back in the laboratory by ICP-MS.
A complementary method was used for determining the ^{234}Th concentration in the water column. Since this same method was also used by another workgroup (Xie & Achterberg) during RV METEOR cruises M136 and M138 (see the corresponding cruise reports), this will yield a considerable dataset for determining the export flux in the Peruvian oxygen minimum zone not only along the transect at 12°S but also further up north along the Peruvian coast.
The method consists in sampling a small volume (4 L) of seawater, in which the total ^{234}Th is co-precipitated with $MnCl_2$ following the addition of a solution of $KMnO_4$. The precipitate is then filtered onto a QMA-filter, which is analyzed for its ^{234}Th beta activity either on board or back in the laboratory. The deployment of in situ pumps is only needed for the collection of particles, in order to determine the C/^{234}Th ratio.
The advantage of the method is the fact that samples can be obtained from CTD-rosette casts, which require much less ship time than in situ pump casts (about 1 hour compared to 3-4 hours) and enable the sampling of up to 24 depths in a single cast. For this cruise, Niskin sampling was done at 2 sites corresponding to in situ pump sampling, the sites at 750 m and 1000 m water depth, and one site at 142 m depth.

Table 5.1.7.1: Sampling overview. No. of samples does not include the ^{238}U samples, of which 10-12 samples were taken at each site. At sites 750 m and 1000 m, no. of samples indicates ISP+ Niskin (small volume). Abbreviation: ISP = in situ pumps.

Site (water depth)	Sampling gear	No. of samples	Parameters measured
74 m	ISP, Niskin	5	^{234}Th (diss. part.), ^{238}U, C_{org}
142 m	Niskin	11	^{234}Th (tot.), ^{238}U
244 m	ISP, Niskin	9	^{234}Th (diss., part.), ^{238}U, C_{org}
400 m	ISP, Niskin	10	^{234}Th (diss., part.), ^{238}U, C_{org}
750 m	ISP, Niskin	9+12	^{234}Th (diss., part., tot.), ^{238}U, C_{org}
1000 m	ISP, Niskin	9+9	^{234}Th (diss., part., tot.), ^{238}U, C_{org}

Bacterial sulfate reduction activity in the water column

Tina Treude

When oxygen is exhausted in the water column, microbial organic matter degradation continues with other electron acceptors. Sulfate is abundantly available in the marine environment and specifically particles (marine snow) could provide metabolic micro-niches for bacterial sulfate reduction. Bacterial sulfate reduction activity was investigated in the water column at different stations and water depths along the 12°S transect by accumulating particles on filters (polycarbonate, diameter 293 mm, pore size 1 µm) using situ pumps (McLane Research Laboratories, Inc.). Water depths were selected according to previous CTD profiles to sample: (1) at the top of the oxic/anoxic transition, (2) within the OMZ, and (3) at the bottom of the anoxic/oxic transition or (if anoxia reached the seafloor) close to the seafloor. After particle accumulation, filters where cut under an anoxic argon atmosphere in a cold room and subsampled for different analytes: sulfate reduction rate measurements, molecular analyzes, and catalyzed reporter deposition fluorescence in situ hybridization (CARD-FISH). Filter samples for sulfate reduction were intermittently stored in sterile-filtered anoxic seawater until they were transferred to the actual incubation vials. Seawater for sulfate reduction incubations and additional analyzes (nutrients, molecular analyzes, CARD-FISH) was retrieved by CTD water sampling rosette from the same stations/depths following the in-situ pump deployments. Filter samples for sulfate reduction determinations were transferred to 30 mL crimp-sealed borosilicate vials filled with the respective in-situ water collected from the CTD/Rosette. Vials were sealed headspace free. Three replicate vials from each water depth were enriched with 13 µM sulfide (approx. final concentration), three replicates remained unchanged, three replicates (just water) were incubated without filter added. To each vial, 1.85 MBq 35S-sulfate radiotracer was injected and vials were incubated for approximately 9 hrs in the dark at 12°C. After incubation, the vials were opened, mixed with 3.5 ml 50% w/v zinc acetate solution, transferred to 50 ml plastic centrifuge vials, and frozen at -20°C. Dead control samples were first mixed with zinc acetate before radiotracer addition. CTD/Rosette water for molecular and CARD-FISH analyses was filtered through 0.2 µm polycarbonate filters to accumulate DNA and cells, respectively. Filters for molecular analyzes (from both in situ pump and CTD water) were directly frozen at -20°C. Filters for CARD-FISH analyses from both in situ pump and CTD water were fixed in 3% formaldehyde and then washed with phosphate buffer saline (PBS) and PBS/Ethanol (1:1) and subsequently stored at -20°C. Analyses of all samples will continue in the shore-based laboratory.

Table 5.1.7.2: Overview of In Situ Pump stations and associated CTD/Rosette stations sampled for water-column sulfate reduction studies.

In Situ Pump Station #	CTD Station #	Water depth at Station (m)	Sampled water depths (m)
652	655 (CTD 18)	244/244	80, 130, 225
694	697 (CTD 35)	128/127	50, 70, 110
719	722 (CTD 45)	74/74	30, 45, 60
750	752 (CTD 56)	262/261	80, 130, 225

5.2 Benthic biogeochmistry

5.2.1 Porewater geochemistry

(A. W. Dale, A. Plass, B. Domeyer, G. Schüssler, M. Paul, K. Meier)

Objectives

The porewater composition of surface sediments was investigated at nine stations at the 12°S transect in order to characterize and quantify sediment diagenetic processes below the oxygen-deficient waters offshore Peru. One aim of this cruise was to further our understanding of the benthic-pelagic coupling in oxygen deficient regions of the ocean by examining key geochemical species whose chemical behaviour and distribution are altered via changes in redox potential. Specific emphasis was placed on the biogeochemical cycling of redox sensitive elements such as N, P and Fe, which are preferentially released from sediments under oxygen deficient bottom waters. The magnitude of this recycling flux, the relative importance of key control parameters, and the coupling to the carbon cycle are still poorly understood. In order to overcome this lack of knowledge, we performed geochemical analyses of pore water from surface sediments that were retrieved by multiple-corer (MUC) and benthic lander deployments (BIGO). We also carried out ex situ whole-core incubations at 200 m and 750 m water depth to better understand the response of sediments under variable redox conditions in the bottom water (see Section 5.2.3).

Methods

Sediment cores (max. ~ 40 cm in length) were retrieved using the multiple-corer (MUC) in addition to smaller push cores recovered with the BIGO landers (max. ~ 15 cm in length). An overview of the sampling stations where porewater was analyzed is given in Table 5.2.1.1. This table also includes sediments that were sampled during the previous cruise M136. After retrieval, all cores were transferred to a cooling lab (12°C, mean bottom water temperature along the transect) and processed within 1-2 hours. Supernatant bottom water of the multiple-cores was sampled and filtered for subsequent analyses. In general, one main MUC was taken at the same site of BIGO deployments, but not necessarily on the same day. Sediment samples from the cores sectioned in the glove bag were spun in a refrigerated centrifuge at 4000 rpm for 20 min to separate the porewater from the particulates. For all measurements and sub-sampling for redox-sensitive parameters (e.g. Fe, nutrients) from the MUC cores, the sediments were sectioned and porewaters sub-sampled in an argon filled glove bag. The sampling depth resolution increased from 1 cm at the surface to 4 cm at depth. Inside the glove bag, porewater samples were filtered with 0.2 nm cellulose-acetate filters. Porewater extraction yielded 20-50 ml of porewater at each depth interval. BIGO cores from the main (non-experimental) lander deployments were sectioned rapidly under ambient atmosphere, centrifuged, and filtered inside the glove bag. Sediment samples were also taken for the calculation of sediment density and water content as well as solid phase constituents in the onshore laboratory.

A total of 691 porewater samples were recovered and analyzed (Table 5.2.1.1). Porewater analyses of the following parameters were carried out on board: ferrous iron (Fe^{2+}), nitrate (NO_3^-), nitrite (NO_2^-), ammonium (NH_4^+), phosphate (PO_4^{3-}), silicate (H_4SiO_4), total alkalinity (TA) and hydrogen sulphide (H_2S). For H_2S analysis, an aliquot of pore water was diluted with appropriate amounts of oxygen-free artificial seawater and the sulphide was fixed by immediate addition of zinc acetate gelatine solution immediately after pore-water recovery. NO_3^- and NO_2^- were determined on a Quaatro Autoanalyzer (Seal Analytic) using standard methods (Grasshoff et al., 1999) with detection limits of 30 and 5 nM set by the lowest calibration standards, respectively. NH_4^+, PO_4^{3-}, H_4SiO_4 and H_2S nitrate were determined on a Hitachi U-2001 spectrophotometer

with detection limits of 2, 5, 1 and 1 µM (respectively). For the analysis of dissolved Fe^{2+} concentrations, sub-samples of 1 ml were taken within the glove bag, immediately stabilized with ascorbic acid and later analysed after complexation with 20 µl of Ferrozin. The precision of this assay was <2 %. Samples for TA were analyzed by titration of 0.5-1 ml pore water according to Ivanenkov and Lyakhin (1978). Titration was ended when a stable pink colour appeared. During titration, the sample was degassed by continuously bubbling nitrogen to remove any generated CO_2 and H_2S. The acid was standardized using an IAPSO seawater solution. The detection limit and precision of the method is 0.05 meq L^{-1}.

Untreated samples were also stored in a refrigerator for onshore analysis of chloride, bromide, and sulphate by ion-chromatography. Acidified sub-samples (3-8 ml with 1% v/v concentrated trace metal grade nitric acid) were prepared for analyses of major ions (K, Li, B, Mg, Ca, Sr, Mn, Br, and I) and trace metals by inductively coupled plasma optical emission spectroscopy (ICP-OES) and inductively coupled plasma mass spectrometry (ICP-MS). Samples for DIC and stable N isotopes (^{15}N, ^{14}N) will also be determined on selected sub-samples in the shore-based laboratories.

Table 5.2.1.1: Stations for geochemical analysis of porewaters from multiple-corer (MUC) and benthic lander (BIGO, chamber 1 (C1) or chamber 2 (C2)) samples listed by water depth. BIGO cores are marked in blue for clarity. The table includes M136 and M137. Note that sediments from 3 stations (338, 342 and 409) were recovered at 14°S, whereas all other deployments were made at 12°S.

Station †	Cruise	Depth (m)	Date (2017)	Lat. [°S]	Long. [°W]	No. samples
483MUC8	M136	74	24-Apr	12°13.519'	77°10.793'	17
426MUC8 (DOM)	M136	74	24-Apr	12°13.519'	77°10.793'	14
533BIGO2-4 C1	M136	74	27-Apr	12°13.499'	77°10.776'	10
614BIGO1-1 C2 *	M137	74	07-May	12°13.514'	77°10.787'	27
739BIGO2-4	M137	75	17-May	12°13.504'	77°10.799'	25
754BIGO1-4 C1 *	M137	75	17-May	12°13.504'	77°10.799'	9
754BIGO1-4 C2 *	M137	75	17-May	12°13.504'	77°10.799'	10
817BIGO2-6 C1 *	M137	75	22-May	12°13.49'	77°10.78'	11
817BIGO2-6 C2 *	M137	75	22-May	12°13.49'	77°10.78'	11
830BIGO1-6 C1 *	M137	75	23-May	12°13.544'	77°10.678'	10
830BIGO1-6 C2 *	M137	75	23-May	12°13.544'	77°10.678'	10
642BIGO2-2 C2	M137	102	09-May	12°14.888'	77°12.699'	11
787MUC33	M137	104	20-May	12°14.80'	77°12.70'	15
577MUC11 (DOM)	M136	105	01-May	12°15.137'	77°12.880'	14
777BIGO2-5 C1 *	M137	127	19-May	12°16.69'	77°14.984'	10
426MUC6	M136	129	19-Apr	12°16.678'	77°14.954'	17
426MUC6 (DOM)	M136	129	19-Apr	12°16.678'	77°14.954'	12
488BIGO2-3 C1	M136	130	25-Apr	12°16.787'	77°15.009'	9
656BIGO1-2 C1 *	M137	130	10-May	12°16.798'	77°14.989'	11
656BIGO1-2 C2	M137	130	10-May	12°16.798'	77°14.989'	10
651MUC8	M137	144	10-May	12°18.709'	77°17.796'	15
651MUC8 (DOM)	M137	144	10-May	12°18.709'	77°17.796'	12
503BIGO1-3 C1	M136	145	26-Apr	12°18.704'	77°17.792'	10
338MUC1	M136	165	12-Apr	13°51.950'	76°28.100'	16
739BIGO2-4	M137	190	16-May	12°21.501'	77°21.708'	25
739BIGO2-4 C1 *	M137	190	16-May	12°21.501'	77°21.708'	8
739BIGO2-4 C2 *	M137	190	16-May	12°21.501'	77°21.708'	7
696BIGO1-3 C1 *	M137	193	13-May	12°21.506'	77°21.706'	9
696BIGO1-3 C2	M137	193	13-May	12°21.506'	77°21.706'	8
471BIGO1-2 C2	M136	195	23-Apr	12°21.514'	77°21.714'	7
692MUC15	M137	195	13-May	12°21.504'	77°21.699'	17
692MUC15 (DOM)	M137	195	13-May	12°21.504'	77°21.699'	12
772MUC28 (R1 and R2) **	M137	195	19-May	12°21.573'	77°21.738'	15
773MUC29 (R3) **	M137	195	19-May	12°21.540'	77°21.633'	
774MUC30 (Control) **	M137	195	19-May	12°21.55'	77°21.60'	15
412MUC5	M136	243	18-Apr	12°23.301'	77°24.182'	18
412MUC5 (DOM)	M136	243	18-Apr	12°23.301'	77°24.182'	12
415BIGO2-1 C1	M136	243	18-Apr	12°23.313'	77°24.172'	7
597BIGO2-1 C2	M137	244	06-May	12°23.365'	77°24.276'	24
595MUC1	M137	246	06-May	12°23.298'	77°24.277'	16
430BIGO1-1 C2	M136	302	19-Apr	12°24.893'	77°26.289'	8
574MUC10 ***	M136	302	01-May	12°24.896'	77°26.284'	30
791BIGO1-5 C1 *	M137	302	20-May	12°24.91'	77°26.29'	10
791BIGO1-5 C2 *	M137	302	20-May	12°24.91'	77°26.29'	9
684BIGO2-3 C1 *	M137	304	12-May	12°24.910'	77°26.279'	9
684BIGO2-3 C2	M137	304	12-May	12°24.910'	77°26.279'	10
342MUC2	M136	311	12-Apr	13°57.355'	76°35.633'	16
444MUC7 **	M136	750	20-Apr	12°31.372'	77°35.004'	39
543MUC9	M136	750	28-Apr	12°31.352'	77°35.013'	14
460BIGO2-2 C1	M136	752	21-Apr	12°31.331'	77°34.986'	9
409MUC4	M136	862	17-Apr	14°02.016'	76°42.300'	8
588MUC12 ****	M136	972	02-May	12°34.836'	77°70.342'	7
545BIGO1-4 C1	M136	984	28-Apr	12°34.886'	77°46.384'	6

† Cores labelled 'DOM' were used for porewater analysis of dissolved organic matter in the onshore laboratory.
* The benthic chambers (C1, C2) corresponding to this core were manipulated geochemically in situ.
** Cores for the incubation experiments at 200 m (control core plus 2 replicates) and 750 m (control core plus 3 replicates).
*** Two cores sectioned from this MUC, with and without a thick surface bacterial mat.
**** Two cores sectioned from this MUC deployment.

Results

Overall, the porewater data resemble the trends observed at the same stations during cruise M92 in 2013 on board RV METEOR (Dale et al., 2016). A notable exception was found for the shallowest station on the shelf (Fig. 5.2.1.1). Whereas in 2013 the surface sediments were covered with thick mats of filamentous sulfide oxidizing bacteria *Thioploca* spp., during M137 the sediments were devoid of conspicuous surface mats. It is striking that the absence of mats is associated with vastly different concentrations of PO_4^{3-}, Fe^{2+} and H_2S in the upper 20 cm, which suggests a direct or indirect role of the bacteria in modulating the levels of these solutes in the porewater. The absence of mats during the present cruise is probably caused by the strong El Niño event in 2015/2016 which is known to ventilate shelf waters and cause a decline in microbial biomass (Gutiérrez et al., 2008). Most likely, a decline in the rate of sulfide oxidation due to the diminished *Thioploca* community explains the build-up of H_2S in the porewater. These data will be further complemented with solid phase analyses and numerical reaction-transport model simulations to quantify the relative importance of *Thioploca* and similar organisms to benthic solute exchange at 12°S on the Peruvian margin (e.g. Bohlen et al., 2011).

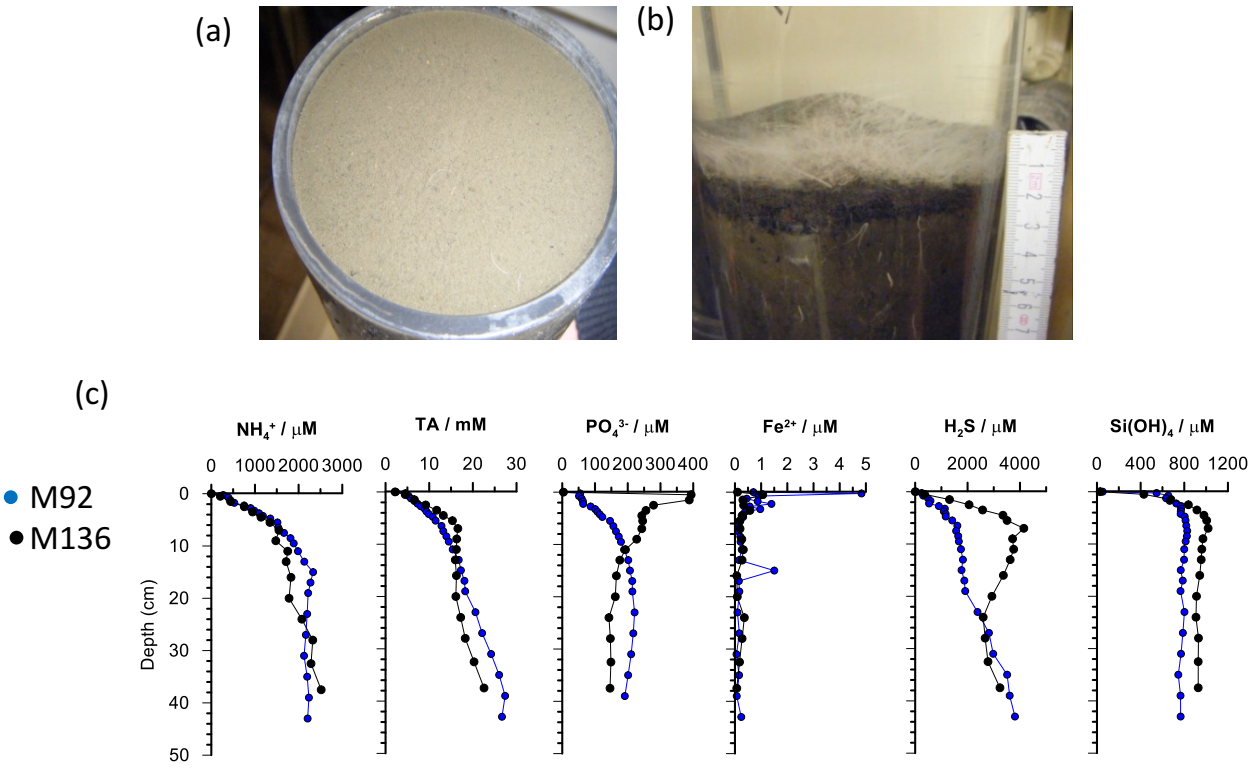

Fig. 5.2.1.1: Photographic images of surface sediments at (a) the shelf station (74 m, 483MUC8), and (b) the same station during M92 in 2013. (c) Measured concentration profiles of dissolved NH_4^+, TA, PO_4^{3-}, Fe^{2+}, H_2S, $Si(OH)_4$ in sediment porewaters sampled by the multi-corer at the shelf station (74 m, 483MUC8) compared to results from the same station during M92 (Dale et al., 2016).

5.2.2 In situ experiments and fluxes

(S. Sommer, J. Braasch, A. Beck, D. Clemens, A. Dale, B. Domeyer, K. Meier, M. Paul, A. Petersen, A. Plaß, G. Schüßler, M. Türk, C. Utecht)

At the beginning of the RV METEOR cruise M137 we finished the in situ natural flux measurements along the 12°S transect, which started during the previous M136 cruise. This includes 3 BIGO deployments at stations at 74 (BIGO-I-1), 102 (BIGO-II-2) and 244 m water depth (BIGO-II-1), (see Chapter 7). Subsequently, the lander program concentrated on in situ experiments testing for the effect of the maintained and elevated availability of nitrate and during one experiment of oxygen on seabed nutrient release using the BIGO type lander.

During natural flux measurements as well as during the experiments, fluxes of oxygen, silicate, sulfide, total alkalinity, dissolved inorganic carbon (DIC), nitrogen species (N_2/Ar, NO_3^-, NO_2^-, NH_4^+), phosphate and trace metals across the sediment water interface were determined in benthic chambers. In addition, the sediments were sampled for pore water geochemistry, physical properties of the sediment (water content, porosity, C, N, S analysis) (see Section 5.2.1), as well as for foraminifera (see Section 5.2.4) and sulfur bacteria. At selected stations samples were taken for dissolved organic matter (DOM) as well as for nitrogen isotopic analyses.

Two structurally similar BIGO´s (BIGO I and BIGO II) were deployed as described in detail by Sommer et al. (2009), Fig. 5.2.2.1A. In brief, each BIGO contained two circular flux chambers (internal diameter 28.8 cm area 651.4 cm^2). A TV-guided launching system allowed smooth placement of the observatories at selected sites on the sea floor. Four hours after the observatories were placed on the sea floor the chambers were slowly driven into the sediment (~ 30 cm h^{-1}). During this initial time period where the bottom of the chambers was not closed by the sediment, the water inside the flux chamber was periodically replaced with ambient bottom water. The water body inside the chamber was replaced once more with ambient bottom water after the chamber has been driven into the sediment to flush out solutes that might have been released from the sediment during chamber insertion. To trace nitrogen fluxes, iron, phosphorous and silicate release as well as total alkalinity 8 sequential water samples were removed with a glass syringe (volume of each syringe ~ 47 ml) by means of glass syringe water samplers, Fig. 5.2.2.1B. The syringes were connected to the chamber using 1 m long Vygon tubes with a dead volume of 5.2 ml. Prior to deployment these tubes were filled with distilled water. Another 8 water samples were taken from inside of one of the two benthic chambers using an eight-channel peristaltic pump, which slowly filled glass tubes (quartz glass), Fig. 5.2.2.1B, C. These samples were used for the gas analyses of N_2/Ar (Sommer et al. 2016) as well as DIC (Sommer et al. 2017). A further set of 8 glass tubes were used to take samples for trace metal measurements from the other chamber. To monitor the ambient bottom water geochemistry an additional syringe water sampler and another series of eight glass tubes were used. The positions of the sampling ports were about 30 – 40 cm above the sediment water interface. O_2 was measured inside the chambers and in the ambient seawater using optodes (Aandera) that were calibrated before each lander deployment.

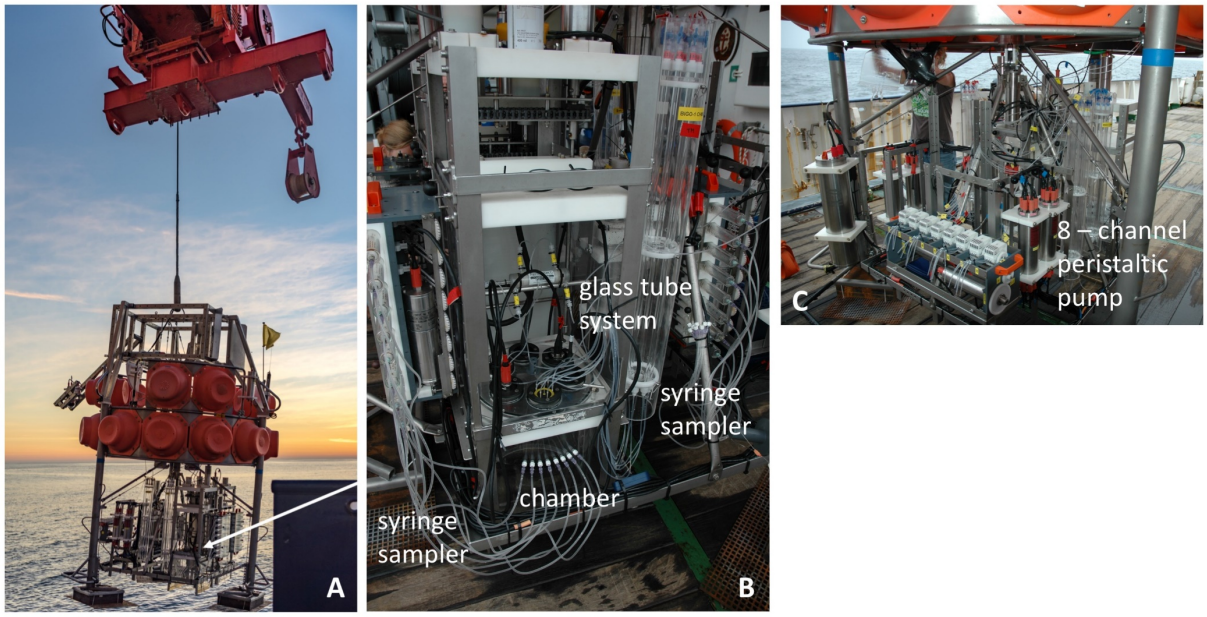

Fig. 5.2.2.1 **A** Lander and Launcher prior to deployment; **B** Flux chamber with attached syringe water sampler and the glass tube system; **C** 8-channel peristaltic pump for taking samples from the chamber and the ambient bottom water into the glass tubes (Photos: A, C. Rohlder, B and C, S. Sommer).

Similar to the previous cruise M136 during this cruise the glass tubes connected to chamber 1 were used for dissolved iron analyses and were filtered (filter sizes 0.2 and 5 µm) whilst sampling. In addition to the chambers and ambient bottom water vertical nutrient gradients were sampled using an arm that extended vertically from the lander into to water column allowing to sample water in vertical heights from the seafloor of 0.5, 1, 2, 3, and 4 m (F. Scholz).

Nine lander-based experiments were conducted on selected stations in water depths of 74, 129, 193 and 302 m. Previous results, which were obtained during M136 and M92 showed that these sites at the shallow shelf and the upper slope are the most active sites with regard to element turnover and nutrient release. These sites were further selected based on the water column geochemistry and on the occurrence of sulfur bacteria and foraminifera. Please note that in contrast to the previous METEOR cruise M92 the shallowest site at 74 m was only scarcely populated with sulfur bacteria, which might be related to the post El Niño conditions.
At each of the experimental sites two BIGO deployments were conducted, Fig. 5.2.2.2. During one lander deployment chamber was used for a control (denoted as C in Fig. 5.2.2.2, no addition of nitrate) and the second chamber for N and P flux measurements under conditions of nitrate addition. Since dissolved iron (denoted as Fe in Fig. 5.2.2.2) as well as the combined N_2/Ar and DIC measurements (denoted as N in Fig. 5.2.2.2) cannot be conducted using the same glass tube water samples, a second lander deployment became necessary. During this deployment nitrate was added into both chambers and the glass tube sampling system was used in one case for N_2/Ar and DIC measurements and the other one for dissolved iron measurements.

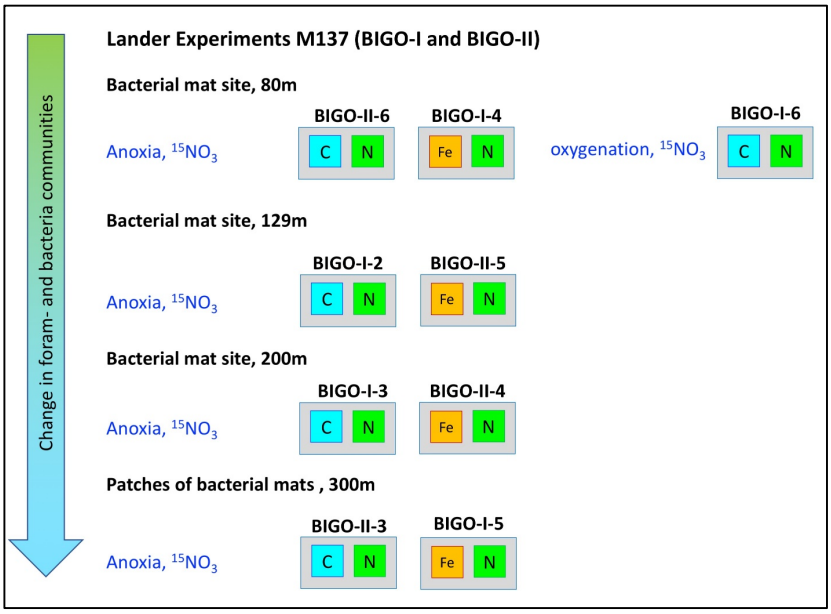

Fig. 5.2.2.2 Scheme of the lander deployments for in situ experiments testing the effect of maintained NO_3^- availability and oxygen on seabed nutrient fluxes. The two chambers per lander are indicated as squares. C: control no addition of NO_3^-. All other chambers were treated with NO_3^- and during BIGO-I-6 deployment with O_2. Whether the glass tube water samples are used for combined N_2/Ar and DIC measurements or dissolved Fe analysis is indicated by N and Fe.

Still small sized NO_3^- sensors are not available, which would allow the construction of a chemostat system allowing the controlled addition of nitrate. Hence, the NO_3^- addition into the chamber was not actively regulated but instead, based on previous NO_3^- uptake measurement respective rates were presumed. Nitrate additions took place using a peristaltic pump. The concentration and volumes of the NO_3- and or ^{15}N-NO_3^- solution added as well as the settings of the pump are given in Table 5.2.2.1

Table 5.2.2.1: Details of nitrate injection during in situ experiments. Conc: Concentration of the injected solution; Steps: Number of steps conducted by the injection pump; Vol: volume per each injection; First: denotes start of the injection, Freg: denotes frequence of injection per hour; Last: time when last injection was performed; Total Volume denotes entire volume of all injection into the benthic chamber.

GEAR	Chamb	Injection Solution	Conc	Steps	Rate	Vol	First	Freq	Last	Total Volume
			mM	No.	µL/step	ml	h	1/h	h	ml
BIGO2-1	Ch1									
	Ch2									
BIGO1-1	Ch1	NO_3 unlabelled	8.065	620	7.2	4.46	1	1	32	142.8
	Ch2	NO_3 unlabelled	8.065	620	7.0	4.34	1	1	32	138.9
BIGO2-2	Ch1									
	Ch2									
BIGO1-2	Ch1	$NO_3 + Na^{15}NO_3$	7.757 *	902	7.2	6.49	0	1	32	214.3
	Ch2									
BIGO2-3	Ch1	$Na^{15}NO_3$	2356.75	695	7.2	5.00	0	1	0	5.0
	Ch2									
BIGO1-3	Ch1	$NO_3 + Na^{15}NO_3$	164.59**	503	7.2	3.52	0	1	32	116.3
	Ch2									
BIGO2-4	Ch1	$Na^{15}NO_3$	0.164	359	7.2	2.58	0	2	32	170.6
	Ch2	$Na^{15}NO_3$	0.164	359	7.0	2.51	0	2	32	165.9
BIGO1-4	Ch1	$Na^{15}NO_3$	0.188	266	7.0	1.86	0	2	32	122.9
	Ch2	$Na^{15}NO_3$	0.188	266	7.2	1.92	0	2	32	126.9
BIGO2-5	Ch1	$Na^{15}NO_3$	0.188	455	7.2	3.28	0	2	32	216.2
	Ch2	$Na^{15}NO_3$	0.188	455	7.0	3.19	0	2	32	210.2
BIGO1-5	Ch1	$Na^{15}NO_3$	1.885	292	7.0	2.04	0	2	32	134.9
	Ch2	$Na^{15}NO_3$	1.885	292	7.2	2.11	0	2	32	139.3
BIGO2-6	Ch1	$Na^{15}NO_3$	38.035	376	7.2	2.71	0	2	32	178.7
	Ch2	$Na^{15}NO_3$	38.035	376	7.0	2.63	0	2	32	173.7
BIGO1-6	Ch1	$Na^{15}NO_3$	38.035	376	7.0	2.63	0	2	32	173.7
	Ch2	$Na^{15}NO_3$	38.035	376	7.2	2.72	0	2	32	179.4

* 50 ‰ delta notation, ** 0.5 atom % otherwise 0.98 atom %

At the shallowest site at 75 m, which experienced fluctuating bottom water O_2 conditions, an oxygenation experiment was conducted providing O_2 by the catalytical cleavage of hydrogen peroxide. Aim was to maintain a minimum O_2 concentration inside the chamber at a level of 30 µM.

Preliminary Results

All experiments were successful, however there were difficulties to keep the NO_3^- level inside the chamber at a constant level. Interestingly, the in-situ chamber experiments indicate that the release of phosphate is linked to the availability of nitrate in the bottom water. At higher nitrate levels the release of phosphate often was found to be suppressed or even uptake of phosphate took place. An example of this is given in Figure 5.2.2.3. during an experiment at 128 m water

depth. The results of the in-situ experiments and those of the ex situ experiments showing a similar behaviour as described above (see Section 5.2.3) will be jointly interpreted.

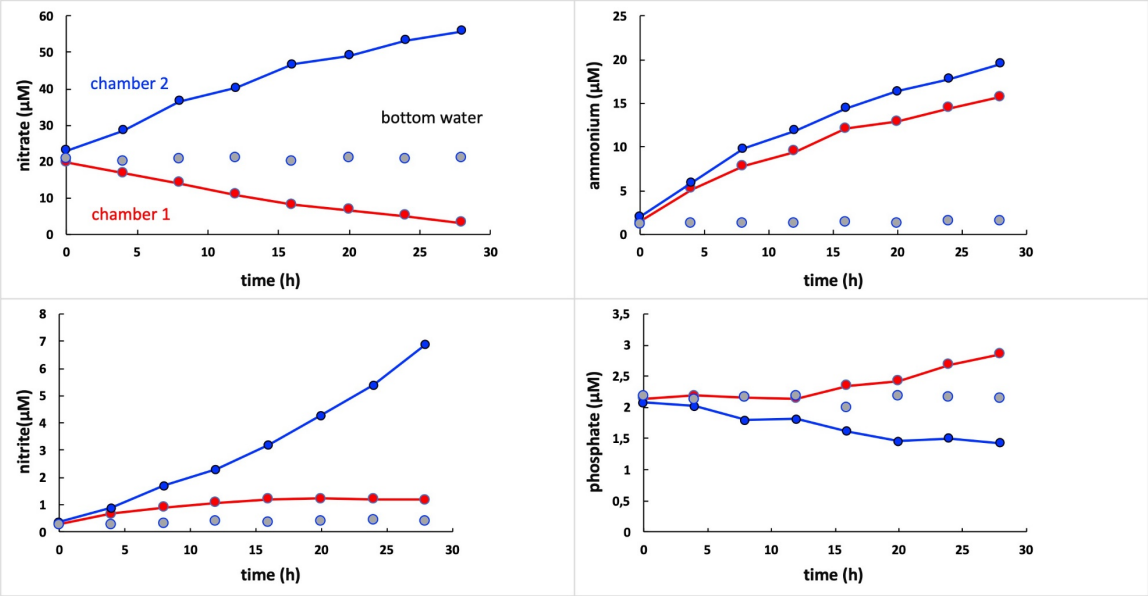

Fig. 5.2.2.3 Concentrations of NO_3^-, NO_2^-, NH_4^+ and PO_4^{3-} over time inside chamber 1 (red points), chamber 2 (blue points) and the ambient bottom water (grey points) during deployment of BIGO-I-2 at 128 m water depth.

Expected results
After the evaluation of the different experiments we expect to better understand the effect of the availability of oxidants on the fluxes of particularly NH_4^+, PO_4^{3-} and dissolved iron. We hope that these analyses allow us to better constrain and close the mass balances for phosphate (Noffke et al. 2012, Lomnitz et al. 2016) or to further investigate the Fe oxidation using nitrate as electron acceptor, which has been determined for the water column (Scholz et al. 2016). In joint synthesis with the natural flux measurements and the water column geochemistry we expect to contribute to a better quantitative understanding of the bentho-pelagic nutrient budget during variable bottom water redox conditions. This in combination with numerical models allows for better up-scaling and predictive capability of benthic-pelagic coupling in the Peruvian OMZ at seasonal and inter-annual time scales as well as during OMZ expansion.

5.2.3 Ex situ experiments

(A.W. Dale, D. Clemens, A. Plass, S. Langer, B. Domeyer, G. Schüssler, R. Surberg, F. Scholz, S. Sommer et al.)

Objectives
At two sites at 12°S (200 m and 750 m), ~30 cm long sediment cores were incubated in the onboard cool room for a period of days to weeks whilst manipulating the redox conditions in the overlying water. The purpose of these experiments was to determine the response of the sedimentary fluxes of dissolved iron, phosphate and nitrogen species to changes in bottom water oxygen and nitrate levels. In addition, at the shallower site, the experiments were targeted to detect changes in the polyphosphate content of large sulfur oxidizing bacteria under these

conditions. The experiments should help to predict how the sediments respond to variable bottom water oxygen and nitrate concentrations that are known to occur in the Peruvian OMZ.

Methods

At two sites at 12°S (200 m and 750 m), 60 cm long core liners (10 cm internal diameter) containing ~30 cm of sediment were recovered, stoppered on deck and transferred to a cool room (7-8°C). The top stoppers were then removed and replaced with PMMA stirring heads with a PVC stirrer bar driven by a rotating magnet inside the head. The cores were sealed and left to settle overnight in darkness, whilst stirring the overlying water at approximately 60 rpm and 15 cm above the sediment surface in darkness. Observed trajectories of small amounts of suspended particulate material at the sediment surface showed that this rate of stirring was sufficient to prevent the formation of a stagnant boundary layer at the interface. Dissolved O_2 concentrations were monitored using Pyroscience oxygen sensor spots ($OXSP_5$) mounted to the inside of the core liners using silicon approximately 15 cm below the top of the liners. O_2 levels were monitored every 10 seconds using fibre optic cables attached to the outside of the core liners opposite the spots using the software Pyro Oxygen Logger.

Exchanging the rubber stopper with the stirrer head inevitably exposes the overlying waters to atmospheric O_2, and concentrations were brought down to in situ levels (~30-40 µM at 750 m, ~0 at 200 m) either by allowing the sediments to respire the O_2 naturally or by bubbling with argon. In each experiment, one core was used as a control by maintaining O_2 and NO_3^- levels as close to ambient levels as possible. Sub-sampling for aliquots of the overlying water (10 ml) was made at regular intervals using a syringe attached to sampling port in the stirrer head via a 5 cm vygon tube. Withdrawal of a sample was compensated by an input of the same volume from a 5 L Supelco inert foil reservoir bag filled with bottom water from the same site and that had been sparged with argon for 30 minutes. The first ml of sample was discarded. NO_3^- levels in the control core continually decreased due to denitrification, which required regular addition of 4.6 ml of 10 mM nitrate stock solution to maintain concentrations at ambient levels. Subsamples were analysed for dissolved Fe^{2+}, NO_3^-, NO_2^-, NH_4^+, PO_4^{3-}, H_4SiO_4, and H_2S. Sub-samples were also taken for dissolved inorganic carbon and ICP-OES. At the end of the experiments, the sediment cores were sectioned under argon as described in Section 5.2.1. Details on chemical analyses made on porewaters and overlying waters are also described in that section. One sediment core was spiked with $H_2{}^{18}O$ to the overlaying bottom water. The sediment with a dense mat of filamentous sulphur bacteria was extruded after one day. Filaments were picked and stored for later analyses by nanoscale secondary ion mass spectrometry (nanoSIMS). This will show whether active cycling of poly-p took place, indicated by oxygen isotope exchange between added $H_2{}^{18}O$ and stored polyphosphate.

Results

A selection of the onboard results from the whole-core incubation experiments at 750 m are shown in in Fig. 5.2.3.1. Dissolved O_2 concentrations in the control were maintained between 15 and 30 µM over the course of the experiment that lasted approximately 25 days. In the other two cores (replicate 1 and 2), O_2 concentrations fell to negligible levels after around 150 d. Approximately, two days later, NO_3^- was exhausted in both replicates and PO_4^{3-} began to accumulate in the overlying water, presumably due to loss of reactive iron oxides at the sediment surface that act as trap for dissolved PO_4^{3-} via adsorption (Slomp et al., 1998). Then, after another two days, Fe^{2+} was lost from the sediment and accumulated to several µM in the overlying water. After ~500 h, PO_4^{3-} in replicate #2 began to level off, with a more gradual decline in Fe^{2+}. This coincided with the addition of NO_3^- to replicate #2, and may imply that nitrate reduction to nitrite followed by in anoxic Fe^{2+} oxidation (Heller et al., 2017) is responsible for the decrease in both Fe^{2+} and PO_4^{3-} (by re-adsorption). Further solid phase

analyses and modelling work will help to elucidate the kinetics of these and other processes more clearly. The results of the ex situ and in situ experiments showing a similar behaviour as described above (see Section 5.2.2) will be jointly interpreted.

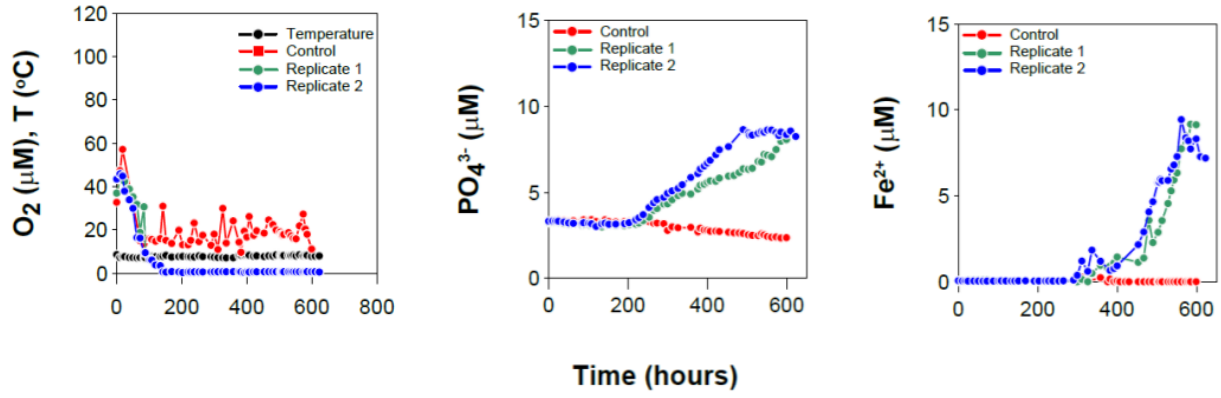

Fig. 5.2.3.1 Time-series of dissolved O_2, PO_4^{3-} and Fe^{2+} in the whole core incubation experiments.

5.2.4 Foraminiferal nitrate respiration in the Peruvian oxygen minimum zone

(N. Glock, A.S. Roy, J. Weißenbach, T. Wein, D. S.R. Chuquival, W.J.C. Bernabe, T. Dagan)

Scientific background

The ability of benthic foraminifera to store and use nitrate as a final electron acceptor was established a few years ago (Piña-Ochoa et al. 2010a, Piña-Ochoa et al. 2010b) and evidences about their involvement in the dissimilatory parts of nitrogen cycle are accumulating (Risgaard-Petersen et al. 2006). The high population density of foraminifera in Oxygen Minimum Zones (OMZ) suggests that they have a prominent role in the biogeochemical nitrogen cycle in these habitats (Bernhard et al. 2012a). Studies performed in the Peruvian OMZ during SFB754 phase II (B7 and B1), revealed that benthic foraminifera are responsible for 40-50% of the total nitrate loss in the OMZ (Glock et al. 2013) and that a hidden nitrate pool, supposedly being maintained by foraminifera (Glud et al. 2009), is present in the uppermost centimetre of near-surface sediments.

Research goals

The main research objective of our project in the Peruvian OMZ was to study the biological and physiological properties of foraminiferal denitrification. Measurements of denitrification, respiration rates and intracellular nutrient storage will further constrain foraminiferal contribution to the benthic nutrient cycling and budgets.

Sampling techniques

Sediment samples were taken with a MUC containing 6 liners and from the benthic lander chambers (BIGO-I and BIGO-II), along a depth transect at 12°S. The top 1 to 3 cm of sediments were sampled and wet sieved directly on board to retrieve benthic foraminifera. Additional samples were taken from the sediment using a 3 cm piston corer and were allocated to immediate preservation for fluorescent in situ hybridization, transmission electron microscopy and Rose Bengal staining. The latter will be used to determine the abundance of live specimen at each station. This information will be used to estimate the total benthic foraminiferal denitrification rates and nutrient storage in the Peruvian OMZ.

Preliminary results

Rates of denitrification and respiration rates were quantified for individual benthic foraminifera by incubation of living specimen in micro-chambers and measuring N_2O production and O_2 consumption with micro-sensors (Piña-Ochoa et al. 2010a). A total of 54 incubations were performed during the cruise. Overall, we determined species-specific denitrification rates for ten species that are abundant in the Peruvian OMZ. Eight of the analysed species were previous unknown to denitrify. Individual denitrification rates were compared with oxygen respiration rates (Fig. 5.2.4.1). The variation of the respiration / denitrification ratio among the species suggests that the denitrification efficiency becomes more important for the organisms with increasing water depth (Fig. 5.2.4.1).

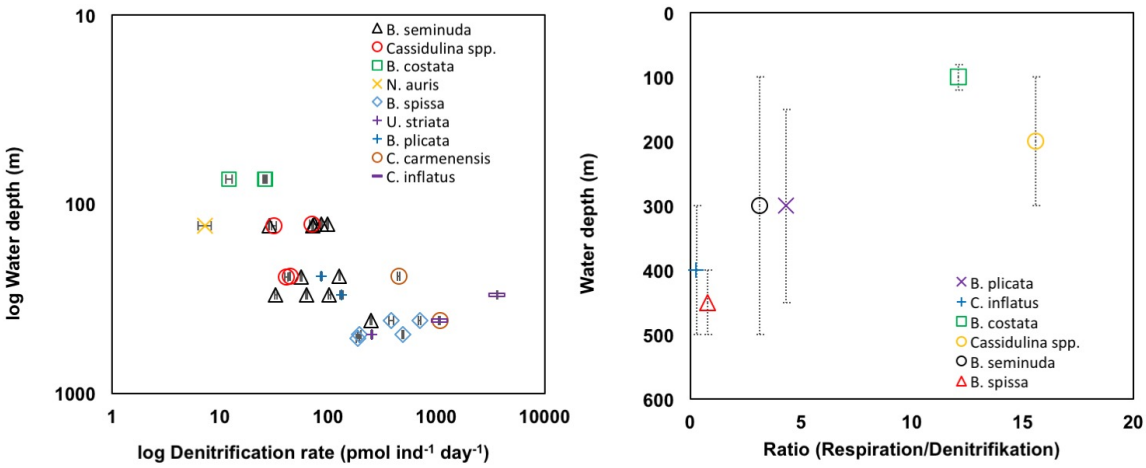

Fig. 5.2.4.1 **Left panel,** Relationship between individual foraminiferal denitrification rates and water depth. **Right panel,** Respiration/denitrification ratio for the most abundant foraminiferal species. Error bars represent the depth distribution of the respective species.

To quantify the intracellular stored nutrients, living foraminifera were cleaned with artificial seawater, frozen in 3 mL of MilliQ water and thawed. Samples were analysed on board using a spectrophotometric auto-analyser (see Section 5.1.4, 5.2.1, 5.2.2). Intracellular NO_3^- storage showed a high intraspecific variability even in replicate cores from the same sampling location. The individual intracellular nitrate storages ranged from 0.05 to 20 nM ind^{-1} and were within the range of previously published data for other foraminifera (Piña-Ochoa et al. 2010a). Furthermore, all analysed specimens showed elevated intracellular phosphate storage. Compared to nitrate the intracellular phosphate concentrations were relatively constant within the same species ranging from 0.07 to 2nM ind^{-1}. These results indicate that benthic foraminifera have a high relevance for the benthic phosphate reservoir, considering their high abundances of up to 600 ind cm^{-2} at the Peruvian OMZ (Glock et al. 2013). Additionally, 28 samples taken from 8 different BIGO deployments (see Section 5.2.2) were frozen using the same procedure but preserved for future analyses. These samples are to be measured for the intracellular content of ^{15}N labelled nitrate from the BIGO incubations to estimate total foraminiferal nitrate uptake rates.

Samples for genomic and transcriptomic sequencing were collected from the MUC at diverse depths. The upper sediment layer was rapidly wet sieved with surface water and directly sorted according to species level under a stereo-microscope. To ensure high transcriptomics quality, the first samples were frozen within less than two hours. Individual life/death state was assessed by analysis of cytoplasm content and colour as well as pseudopodia activity. The life status evaluation was guided by pre-determined life/dead appearance of each species based on a fluorescence analysis. The fluorescence analysis was done at the first day of the cruise and

repeated for any species or station as required. The fluorescence analyses were performed by exposing the foraminifera for about 12hr to a dye that only stains active cell while not being toxic nor affecting individual health (CellTracker™ Green, ThermoFisher Scientific). Guidelines about cytoplasm appearance were determined accordingly for each species to represent living specimen.

Ten different species were sampled for genomics and transcriptomics. Individual samples consist of up to 160 specimens placed in a cryo vial (2 ml, RNAse free) and frozen in liquid nitrogen. In total, 28,566 foraminifera were picked, cleaned and frozen for later analyses. This collection will be used to establish a comprehensive genomic and transcriptomic database of denitrifying foraminiferal species from the Peruvian OMZ. An overview of the amount of picked specimen is presented in Table 5.2.4.1.

Table 5.2.4.1 Collected foraminifera specimens

Species	Total number	Transcriptomic
Bolivina seminuda	8,769	1,298
Cassidulina spp.	6,956	770
Bolivina costata	3,803	674
Bolivina plicata	3,288	173
Uvigerina spp.	2,004	55
Bolivina spissa	1,216	101
Cancris inflatus	1,140	67
Cancris carmenensis	466	70
Nonionella stella	393	80
Globobulimina pacifica	197	0

Additionally, foraminifera of all these species were also sampled for fluorescent in situ hybridization as well as other microscopy techniques including transmission electron microscopy, cryo-scanning electron microscopy, fluorescence and confocal laser scanning microscopy using DAPI and mitotracker staining.

Expected Results

The data we collected will be used to estimate the total benthic foraminiferal nitrate uptake, denitrification rates and total nitrate and phosphate storage in the Peruvian OMZ. The results will be compared to the list of genes and species, which will be obtained from genomics and transcriptomics analyses. Genomic data will be available after nucleic acid extraction and preparation for next generation libraries. These analyses will supply candidate genes involved in the denitrification encoded in foraminifera or the associated bacteria. Samples intended for microscopy, e.g. TEM, CLSM and FISH will be used to visualise presence or absence of microbial endobionts and the mitochondria distribution within the cell.

5.2.5 Polyphosphate in filamentous sulphur bacteria

(S. Langer, A.W. Dale, H.N. Schulz-Vogt, S. Sommer)

Objectives

Some genera of the family *Beggiatoaceae* (filamentous sulphur bacteria) are known for the accumulation of excess phosphate, which is stored as intracellular high energetic polyphosphate (poly-p). This can increase the redox sensitive sedimentary phosphorus pools and might additionally contribute to sedimentary phosphate flux to the bottom water. Shelf and upper slope areas of the Peruvian oxygen minimum zone are inhabited by dense mats of filamentous sulphur bacteria (Gutiérrez et al. 2008, Mosch et al. 2012). However, their contribution to the benthic phosphate flux was treated controversially. An earlier study (Noffke et al. 2012) speculated whether excess P fluxes are caused by widespread filamentous sulphur bacteria, not further specifying which specific group is driving this process. A recent study linked excess sedimentary phosphate fluxes to the presence of members of the family *Marithioploca* (Lomnitz et al., 2016) even if those bacteria were reported to not store poly-p (Høgslund et al., 2009). The main objectives of this study were to prove the presence of poly-p in filamentous sulphur bacteria in the Peruvian OMZ, identify the responsible organisms and quantify the potential phosphorus pool being stored as poly-p.

Methods

Surface sediments obtained by MUC coring between 77 m and 350 m depth were screened for filamentous sulphur bacteria of the genera *Beggiatoa* spp. and *Marithioploca*. Single filaments were stained with the fluorescent dye DAPI, which binds to poly-p when applied at high concentrations (Aschar-Sobbi et al., 2008) and shifts the fluorescence to a higher wavelength. Thus, polyphosphates are discernible as green/ yellow signals under the florescent microscope. As expected from previous studies, *Marithioploca* did not show poly-p inclusions and were therefore not further investigated. Triplicates of 100 filaments of *Beggiatoa* spp. were picked per station and were frozen for later poly-p quantification in the lab (Martin & van Mooy, 2013). Filament lengths and diameters of at least 150 filaments from the same stations were measured for biomass determination. In addition, filaments with different diameters were frozen for sequencing and phylogenetic classification. Ex situ incubation experiments with $H_2{}^{18}O$ aimed to show active poly-p cycling (see Section 5.2.3).

Results

Fluorescence microscopy of DAPI stained filaments confirmed the findings of earlier studies with no poly-p being present in *Marithioploca*. The filaments attributed to *Beggiatoa* spp., however, contained considerable amounts of poly-p based on microscopy. Two filaments with different diameter and different types of poly-p inclusions are shown in figure 5.2.5.1. The left panel shows a filament with a diameter of around 5 µm and poly-p granules of close to 3 µm diameter being present in every cell of the filament. The big poly-p inclusions resemble those found for the cultured *Beggiatoa* strain 35Flor (Brock et al., 2012). In contrast, small (0.5 µm diameter) and unevenly distributed poly-p granules were found in bigger filaments with a diameter of 15 µm (left panel), indicating different poly-p storage mechanisms between different genera of *Beggiatoaceae*.

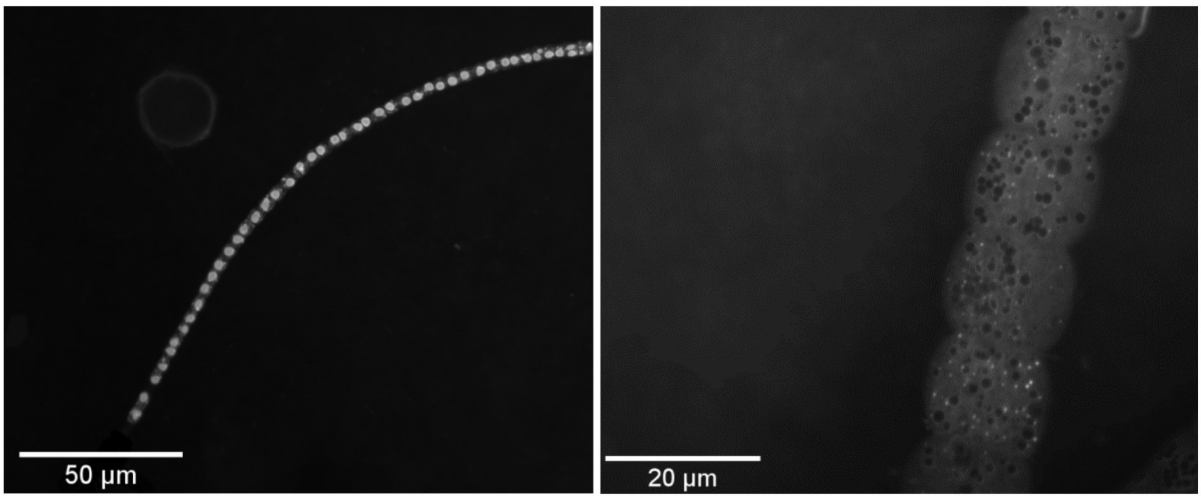

Fig. 5.2.5.1 Poly-p granules visible as bright white spots within the filaments of *Beggiatoa* spp. Left panel: Filament with small diameter and big poly-p globules in every cell. Right panel: Filament with wider diameter and unevenly distributed small poly-p inclusions.

Filament diameter distribution used for biomass calculation of *Beggiatoa* spp. differed between stations, Fig. 5.2.5.2. Diameters between 7.5 and 12 µm were most abundant at the shallowest station at 77 m depth. The station at 244 m showed a dominance of thin filaments with 2.5 µm diameter. Sediments of the stations in between showed high abundances of both size classes (2.5 µm and 7.5 to 10 µm diameter). The calculated biomass together with quantified polyphosphate content will allow the estimation of the relative importance of this transient and redox-sensitive phosphorus pool to the overall benthic P dynamics in the Peruvian OMZ. This analysis will also consider the novel finding of elevated intracellular phosphate storage in foraminifera (see Section 5.2.4).

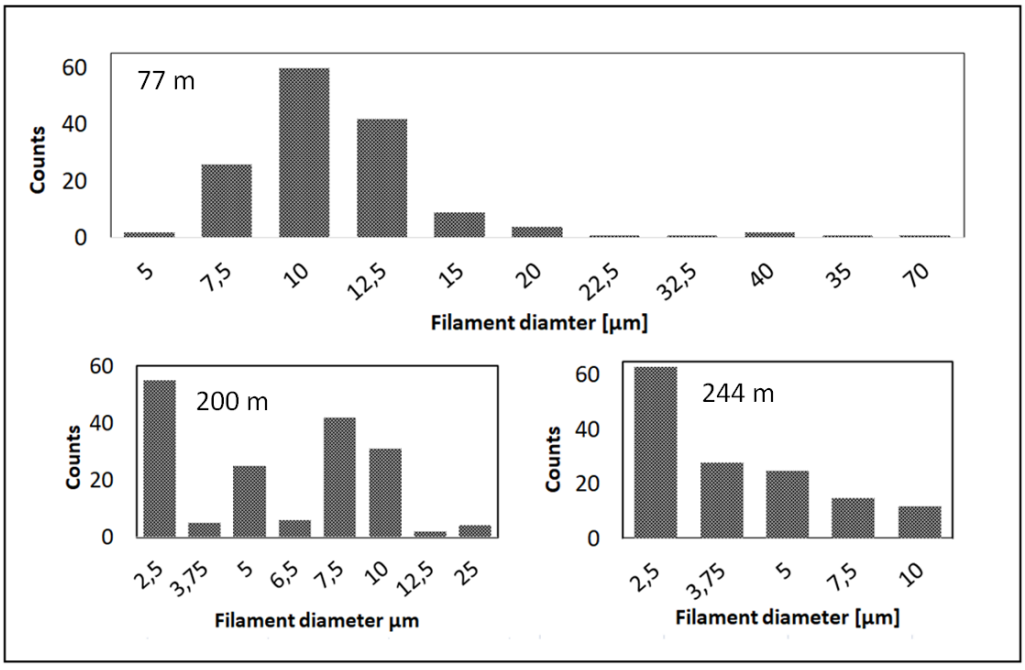

Fig 5.2.5.2 Filament diameter of *Beggiatoa* spp. at various water depths

5.2.6 Sulfate reduction in sediments

(T. Treude)

Bacterial sulfate reduction in the sediment was studied at four multicorer stations along the 12°S transect to compare with water column sulfate reduction (see section 5.1.6). One multicorer core per station was sub-sampled with two small polycarbonate core liners (inner diameter 26 mm, length 20 cm). One small core was injected with sulfide to reach a final sulfide concentration of approx. 10 mM in the porewater. Both small cores were then injected with 1.85 MBq ^{35}S-sulfate radiotracer in 1-cm depth increments through silicon-filled openings. The cores were incubated for approx. 6 hrs in the dark at 12°C. After incubation, cores were sliced in 1-cm increments and slices were each transferred to 50 ml plastic centrifuge tubes filled with 20 ml 20% (w/v) zinc acetate and frozen at -20°C. Dead controls were first transferred to zinc acetate before radiotracer addition. One multicorer core per station was subsampled (0-5 cm, homogenized) for molecular analyzes. Samples were frozen at -20°C. Analyzes of all samples will continue in the shore-based laboratory.

Table 5.2.6.1 Multicorer stations sampled for sediment sulfate reduction studies.

Station #	MUC #	Water Depth (m)
670	12	752
681	13	74
771	27	128
775	31	243

5.4 Expected Results

(S. Sommer, M. Dengler)

All planned measurements and investigations were conducted successfully. According to the cruise proposals, between the cruises M136 and M137 the composition of the scientific team changed and during cruise M137 a major focus was laid on in situ and ex situ experiments to identify the contribution of sulfur bacteria to the benthic nitrogen cycle and other associated major elements in contrast to foraminifera. The oceanographical measurements in the water column (physics, biogeochemistry), which started on the previous cruise M136 were continued addressing intra-seasonal variability. In order to allow for comparison with the previous SFB cruise M92, which took place in austral summer (Jan.-Feb. 2013) and was characterized by a sulfidic event, nearly all measurements of M136 and M137 were conducted according to a spatially coherent sampling scheme. Furthermore, this cruise was embedded into a series of further Pacific cruises M77, M90, M91, M93, M135 and M138 that took place within the framework of the SFB754.

Altogether, these cruises cover a wide temporal range comprising specific hydrographic and climatological conditions such as the stagnant period encountered during M92 leading to a sulfidic event or conditions of a coastal El Niño with passage of a Kelvin wave (M136 / M137) leading to changes in the velocity of the Peruvian undercurrent and associated changes in the availability of electron acceptors in the bottom water. The combined synthesis of the different results obtained during these cruises allows a better understanding of drivers and consequences of variability in the Peruvian OMZ, which represent a central research topic of the Kieler SFB754.

More specifically, results were obtained to address the following scientific questions or issues:

i. The successful completion of in situ experiments and ex situ whole core experiments in combination with natural flux measurements will contribute to resolve magnitude and pathways of benthic nutrient fluxes (N, P, Fe other trace metals) in response to enhanced availability of NO_3^- and O_2. It is to expect that these findings when linked to time series of O_2 and nutrients allow for better upscaling and predictive capability of the benthic-pelagic coupling in the Peruvian OMZ.
ii. The extended series of ex situ incubations of selected foraminiferal species to determine their O_2 and nitrate uptake will strongly help to address the extent to which benthic N, P and S-fluxes are coupled and controlled by filamentous sulfide oxidizing bacteria *Beggiatoa* and *Thioploca* as well as by denitrifying foraminifera. A first study addressing NO_3^- and oxygen uptake by Foraminifera has been published in PNAS (Glock et al.(2019) Metabolic preference of nitrate over oxygen as an electron acceptor in Foraminifera from the Peruvian oxygen minimum zone.
iii. On board investigations jointly conducted with the Institute for Baltic Sea Research, Warnemünde (H.N. Schulz-Vogt, S. Langer) will further contribute to identify sulfur bacteria capable for polyphosphate storage and to get insight into the dynamics of polyphosphates in sulfur bacteria. These microbial activities are suspected to affect transient release and uptake of phosphate under different bottom water redox conditions modulating benthic P fluxes.
iv. The multi-cruise physical and biogeochemical measurement program within the SFB framework provide the unique opportunity to address intra-seasonal, seasonal and inter-annual variability in physical forcing on the water column biogeochemistry and benthic pelagic coupling. Measurement series were obtained during austral summer in 2008/09 and 2012/13 and compared to austral autumn (M136/M137 2017), which was superimposed by a declining Coastal El Niño event.
v. The investigations during M136/M137 allows to quantify benthic and pelagic cycling of nutrients and trace metals in the OMZ by budgeting physical fluxes of solutes including turbulent fluxes, lateral-diffusive fluxes and advective fluxes in the water column combined with benthic flux measurements. These measurements contribute to address the hypothesis that reduced turbulent mixing occurs during the austral autumn/winter period, which is likely reduces availability of nutrients to the benthic communities and thus reduces benthic turnover rates compared to the austral summer period.
vi. Lastly, during M136/M127 we had the opportunity to observe the offshore propagation of a freshly generated eddy and an associated phase of weak poleward flow. The data will contribute to a better understanding of offshore transport of upwelled nutrients.

6 Ship´s Meteorological Station

(C. Rohleder, M. Knobelsdorf)

In the morning of the 06th of May 2017 RV METEOR left the harbor of Callao under an overcast sky. The wind blew with 3 to 4 Bft from southeast and minor fog patches reduced the visibility mainly along the coast.

The research area was quickly reached as it was only a few sea miles to the southwest of Lima on the northern fringe of an extensive subtropical high over the South Pacific. Hence a southeasterly to southerly airstream persisted with a quite stable air mass developing over the cooler upwelling water close to the coast. The first days of the journey were characterized as mostly cloudy and hazy mornings with mostly sunny afternoons developing. The swell and sea state reached up to 1 to 2 meter.

Until the middle of the first week a trough developed from a tropical trough in the north to a low close to 30°S 83°W. In the research area a low pressure gradient persisted with only light winds however local land/onshore wind circulations dominated the day for wind direction and speed. During the following days the low moved southwards and the subtropical high extended to the east. Therefore, at the beginning of the second week of the expedition mostly southerly and southeasterly winds were experienced.

At the same time an intense low pressure system moved to the south of the subtropical high to the east. In the second half of the week the associated south-southwesterly swell reached the research area of RV METEOR. The freshened southeast trade winds enhanced the average significant wave height to 3 to 4 meter. A cross sea developed and hampered the navigation of the ship. The counter current flow of the surface water even enhanced this effect. During the weekend wind and sea gradually decreased and from the beginning of the third week of the journey calm conditions with winds about 3 Bft and a sea of 2 meters set in. Apart from an increase of the wind on Friday and Saturday the weather pattern did not change much in the last week. During the entire journey precipitation did not have any effect on the weather. The very persistent trade inversion and the relatively cold water in the research area prevented almost any convective processes. On the 21th and 24th observed precipitation had been so little that not even the highly sensitive precipitation sensors were able to catch it. In the night to the 26th it rained again, this time 0.7mm were measured.

In the morning of the 29th of May 2017. RV Meteor reached the harbor of Callao. During this expedition the weather conditions didn’t prevent scientific measurements.

7 Station List M137

Station #	Date	Time (UTC)	Gear #	Latitude	Longitude	Depth (m)	Remarks
M137 - 594	06.05.17	17:29	CTD 01	12°23.30'S	77°24.27'W	244	nutrients
M137 - 595	06.05.17	18:45	TV-MUC 011	12°23.29'S	77°24.27'W	246	
M137 - 596	06.05.17	19:14	MSS 01	12°23.34'S	77°24.29'W	244	
M137 - 597	06.05.17	21:24	BIGO-II-1	12°23.36'S	77°24.276'W	244	deployment
M137 - 598	06.05.17	23:35	CTD 02	12°15.125'S	77°12.931'W	108	nutrients
M137 - 599	07.05.17	00:44	MSS 02	12°15.219'S	77°18.000'W	107	
M137 - 600	07.05.17	02:11	CTD 03	12°16.716'S	77°14.993'W	130	nutrients
M137 - 601	07.05.17	03:09	MSS 03	12°16.896'S	77°15.206'W	128	
M137 - 602	07.05.17	04:30	RAP CST 01	12°28.959'S	77°32.032'W	131.2	end of transect
M137 - 603	07.05.17	06:55	MSS 04	12°30.387'S	77°34.838'W	682	
M137 - 604	07.05.17	08:02	CTD 04	12°31.486'S	77°35.002'W	757	nutrients
M137 - 605	07.05.17	13:12	CTD 05	12°23.298'S	77°25.282'W	243	
M137 - 606	07.05.17	13:30	MUC 02	12°23.299'S	77°24.282'W	244	
M137 - 607	07.05.17	14:14	MUC 03	12°23.297'S	77°24.283'W	245	
M137 - 608	07.05.17	14:53	MUC 04	12°23.257'S	77°24.282'W	244	
M137 - 609	07.05.17	15:38	MUC 05	12°23.323'S	77°24.293'W	243	2nd worked
M137 - 610	07.05.17	16:00	RAP CST 02	12°12.889'S	77°10.642'W	244	end/mid transect74m
M137 - 611	07.05.17	18:22	MSS 05	12°12.932'S	77°10.649'W	69	
M137 - 612	07.05.17	19:04	CTD 06	12°13.490'S	77°10.782'W	74.5	nutrients
M137 - 613	07.05.17	20:12	TM CTD 68	12° 13.48' S	77° 10.81' W	76.4	
M137 - 614	07.05.17	21:47	BIGO-I-1	12°13.514'S	77°10.787'W	74	deployment
M137 - 615	07.05.17	22:16	FISH	12° 13.21' S	77° 11.22' W	74.4	
M137 - 616	07.05.17	22:34	MSS 06	12°13.052'S	77°11.796'W	77	
M137 - 617	07.05.17	23:39	CTD 07	12°14.296'S	77°11.954'W	90	nutrients
M137 - 618	08.05.17	00:07	RAP CST 03	12°14.296'S	77°11.954'W	94.2	start / end of transect
M137 - 619	08.05.17	02:00	MSS 07	12°13.820'S	77°29.152'W	170	
M137 - 620	08.05.17	03:21	CTD 08	12°15.699'S	77°29.529'W	181	nutrients
M137 - 621	08.05.17	03:50	RAP CST 04	12°15.099'S	77°29.529'W	181	start transect coast
M137 - 622	08.05.17	06:19	MSS 08	12°26.01'S	77°12.63'W	166	
M137 - 623	08.05.17	07:15	CTD 09	12°27.152'S	77°12.611'W	179	nutrients
M137 - 624	08.05.17	09:04	MSS 09	12°20.341'S	77°21.669'W	183	
M137 - 625	08.05.17	09:59	CTD 10	12°21.150'S	77°21.754'W	190	nutrients
M137 - 626	08.05.17	13:05	BIGO-II-1	12° 23.20' S	77° 24.24' W	241.1	recovery
M137 - 627	08.05.17	14:30	ISP 01	12° 23.53' S	77° 24.47' W	250.5	
M137 - 628	08.05.17	20:27	RAP CST 05	12°22.577'S	77°56.584'W	253	
M137 - 629	08.05.17	21:22	Glider IFM09	12° 21.86' S	77° 59.80' W	1826.8	recovery
M137 - 630	08.05.17	22:04	TM CTD 69	12°21.84'S	77°59.86'W	1840	
M137 - 631	09.05.17	02:01	MSS 10	12°33.748'S	77°40.507'W	1000	
M137 - 632	09.05.17	03:11	CTD 11	12°35.432'S	77°40.539'W	1020	nutrients
M137 - 633	09.05.17	05:43	MSS 11	12°28.140'S	77°32.299'W	523	
M137 - 634	09.05.17	06:52	CTD 12	12°29.13'S	77°32.98'W	526.7	nutrients

Station #	Date	Time (UTC)	Gear #	Latitude	Longitude	Depth (m)	Remarks
M137 - 635	09.05.17	09:10	MSS 12	12°20.51'S	77°21.23'W	180.5	
M137 - 636	09.05.17	09:36	CTD 13	12°20.76'S	77°21.32'W	183.1	nutrients
M137 - 637	09.05.17	13:00	BIGO-I-1	12°13.38’S	77°10.70’W	72.8	recovery
M137 - 638	09.05.17	13:54	TM CTD 70	12°13.495'S	77°10.785'W	74	
M137 - 639	09.05.17	14:30	ISP 02	12°13.46'S	77°10.75'W	74	
M137 - 640	09.05.17	18:55	MUC 06	12°16.677'S	77°14.993'W	128	
M137 - 641	09.05.17	19:45	MUC 07	12°16.676'S	77°14.994'W	128.4	
M137 - 642	09.05.17	22:13	BIGO-II-2	12°14.888'S	77°12.699'W	102	deployment
M137 - 643	09.05.17	23:09	MSS 13	12°17.325'S	77°17.652'W	136	
M137 - 644	10.05.17	00:32	CTD 14	12°19.220'S	77°17.877'W	148	nutrients
M137 - 645	10.05.17	01:58	MSS 14	12°23.705'S	77°25.951'W	280	
M137 - 646	10.05.17	03:01	CTD 15	12°24.895'S	77°26.257'W	300	nutrients
M137 - 647	10.05.17	04:26	MSS 15	12°28'80'S	77°32.19'W	489	
M137 - 648	10.05.17	05:27	CTD 16	12°29.635'S	77°32.86'W	533.7	nutrients
M137 - 649	10.05.17	06:57	MSS 16	12°26.22'S	77°28.95'W	403.1	
M137 - 650	10.05.17	08:15	CTD 17	12°27.15'S	77°29.50'W	404.9	nutrients
M137 - 651	10.05.17	13:08	MUC 08	12°18.709'S	77°17.796'W	144	
M137 - 652	10.05.17	17:30	ISP 03	12°23.380'S	77°24.135'W	244	
M137 - 653	10.05.17	18:27	TM CTD 71	12° 23.35' S	77° 24.20' W	242.6	
M137 - 654	10.05.17	19:37	MUC 09	12°23.351'S	77°24.251'W	244	
M137 - 655	10.05.17	20:22	CTD 18	12°23.275'S	77°24.358'W	244	
M137 - 656	10.05.17	23:00	BIGO-I-2	12°16.798'S	77°14.989'W	129.4	deployment
M137 - 657	10.05.17	23:34	CTD 19	12°16.708'S	77°14.960'W	128	
M137 - 658	11.05.17	00:37	MSS 17	12°18.567'S	77°19.868'W	156	
M137 - 659	11.05.17	01:56	CTD 20	12°20.170'S	77°19.910'W	170	nutrients
M137 - 660	11.05.17	03:45	MSS 18	12°32.563'S	77°21.511'W	378	
M137 - 661	11.05.17	04:45	CTD 21	12°33.846'S	77°21.610'W	417	nutrients
M137 - 662	11.05.17	06:51	MSS 19	12°26.90'S	77°29.29'W	381	
M137 - 663	11.05.17	07:33	CTD 22	12°26.98'S	77°29.54'W	401	nutrients
M137 - 664	11.05.17	09:20	CTD 23	12°26.87'S	77°36.48'W	446	nutrients
M137 - 665	11.05.17	09:49	MSS 20	12°29.90'S	77°36.49'W	447	
M137 - 666	11.05.17	13:21	BIGO-II-2	12°14.78' S	77°12.59' W	102.5	recovery
M137 - 667	11.05.17	14:33	MUC 10	12°16.821'S	77°15.012'W	128	
M137 - 668	11.05.17	15:08	MUC 11	12°16.845'S	77°15.021'W	129	
M137 - 669	11.05.17	19:00	ISP 04	12°23.50'S	77°23.96'W	244	
M137 - 670	11.05.17	23:22	MUC 12	12°31.358'S	77°34.997'W	752	
M137 - 671	12.05.17	01:15	TM CTD 72	12°36.573'W	77°43.051'W	1070	
M137 - 672	12.05.17	04:23	CTD 24	12°15.016'S	77°43.999'W	1400	
M137 - 673	12.05.17	05:32	CTD 25	12°12.03'S	77°39.98'W	1019	nutrients
M137 - 674	12.05.17	06:32	CTD 26	12°11.06'S	77°38.63'W	707	
M137 - 675	12.05.17	07:27	CTD 27	12°10.07'S	77°37.30'W	337	
M137 - 676	12.05.17	08:16	CTD 28	12°09.03'S	77°35.75'W	197	
M137 - 677	12.05.17	09:06	CTD 29	12°07.52'S	77°33.92'W	165	

Station #	Date	Time (UTC)	Gear #	Latitude	Longitude	Depth (m)	Remarks
M137 - 678	12.05.17	09:53	CTD 30	12°06.02'S	77°31.98'W	154	nutrients
M137 - 679	12.05.17	10:20	RAP CST 06	12°06.09'S	77°31.91'W	154	software problems
M137 - 680	12.05.17	13:15	BIGO-I-2	12°16'372'S	77°14.952'W	128	recovery
M137 - 681	12.05.17	17:36	MUC 13	12°13.507'S	77°10.774'W	74.2	
M137 - 682	12.05.17	18:04	MUC14	12'13.497'S	77°10.787'W	75	
M137 - 683	12.05.17	19:38	CTD 31	12°16'784'S	77°14.982'W	127	
M137 - 684	12.05.17	22:31	BIGO-II-3	12°24.90'S	77°26.29'W	302	deployment
M137 - 685	13.05.17	02:20	TM CTD 73	12°39.50'S	77°47.03'W	1446	
M137 - 686	13.05.17	03:15	MSS 21	12°39.489'S	77°47.128'W	1451	
M137 - 687	13.05.17	04:30	CTD 32	12°39.492'S	77°47.103'W	1446	nutrients
M137 - 688	13.05.17	06:25	MSS 22	12°36.59'S	77°43.34'W	1076	
M137 - 689	13.05.17	07:16	CTD 33	12°37'16'S	77°43.60'W	1121	nutrients
M137 - 690	13.05.17	09:15	MSS 23	12°32.51'S	77°37.42'W	919	
M137 - 691	13.05.17	10:03	CTD 34	12°33.44'S	77°37.76'W	955	nutrients
M137 - 692	13.05.17	13:20	MUC 15	12°21.504'S	77°21.699'W	194	
M137 - 693	13.05.17	14:05	MUC 16	12°21.499'S	77°21.702'W	195	
M137 - 694	13.05.17	18:00	ISP 5	12°16.78'S	77°14.98'W	128	
M137 - 695	13.05.17	18:42	MUC 17	12°16.780'S	77°14.979'W	130	
M137 - 696	13.05.17	21:08	BIGO-I-3	12°21.506'S	77°21.706'W	193	deployment
M137 - 697	13.05.17	22:20	CTD 35	12°16.759'S	77°14.964'W	127	
M137 - 698	13.05.17	22:39	RAP CT 07	12°16.86'S	77°15.01'W	128	
M137 - 699	14.05.17	03:15	TM CTD 74	12°43.03'S	77°50.03'W	2060	
M137 - 700	14.05.17	04:46	MSS 24	12°43.13'S	77°50.07'W	2058	
M137 - 701	14.05.17	05:39	CTD 36	12°44.00'S	77°50.10'W	2135	nutrients
M137 - 702	14.05.17	13:01	BIGO-II-3	12° 24.84' S	77° 26.23' W	300.8	recovery
M137 - 703	14.05.17	15:00	ISP 06	12°27.21'S	77°21.59'W	408	
M137 - 704	14.05.17	19:19	MUC 18	12°29.280'S	77°32.267'W	507	empty
M137 - 705	14.05.17	20:23	MUC 19	12°28.923'S	77°31.684'W	476	empty
M137 - 706	14.05.17	21:00	RAP CST 08	12°28.59'S	77°32.24'W	491	
M137 - 707	15.05.17	00:00	CTD 37	12°19.950'S	78°03.144'W	1967	nutrients
M137 - 708	15.05.17	00:50	TM CTD 75	12°19.95'S	78°03.06'W	1966	
M137 - 709	15.05.17	02:18	MSS 25	12°20.06'S	78°03.35'W	1990	
M137 - 710	15.05.17	03:55	CTD 38	12°19.981'S	77°58.019'W	1718	nutrients
M137 - 711	15.05.17	05:18	CTD 39	12°20.022'S	77°52.011'W	1582	
M137 - 712	15.05.17	07:09	CTD 40	12°19.56'S	77°45.88'W	1398	nutrients
M137 - 713	15.05.17	08:31	CTD 41	12°20.02'S	77°39.96'W	1048	
M137 - 714	15.05.17	09:36	CTD 42	12°20.01'S	77°36.93'W	463	
M137 - 715	15.05.17	10:23	CTD 43	12°20.02'S	77°33.92'W	374	nutrients
M137 - 716	15.05.17	11:30	CTD 44	12°20.05'S	77°27.88'W	239	nutrients
M137 - 717	15.05.17	13:37	BIGO-I-3	12°21.486'S	77°21.714'W	195	recovery
M137 - 718	15.05.17	14:05	MUC 20	12°21.488'S	77°21.707'W	195	
M137 - 719	15.05.17	16:00	ISP 07	12°13.44'S	77°10.79'W	74	
M137 - 720	15.05.17	19:15	MUC 21	12°13.47'S	77°10.787'W	75	

Station #	Date	Time (UTC)	Gear #	Latitude	Longitude	Depth (m)	Remarks
M137 - 721	15.05.17	19:35	MUC 22	12°13.470'S	77°10.797'W	75	
M137 - 722	15.05.17	20:14	CTD 45	12°13.295'S	77°10.826'W	74	
M137 - 723	15.05.17	20:45	MSS 26	12°13.053'S	77°10.591'W	70	
M137 - 724	15.05.17	21:55	CTD TM 76	12°13.45'S	77°10.83'W	74	
M137 - 725	15.05.17	22:20	CTD 46	12°13.535'S	77°10.801'W	75.2	nutrients
M137 - 726	15.05.17	22:59	MSS 27	12°13.01'S	77°11.64'W	75	
M137 - 727	16.05.17	00:11	CTD 47	12°14.235'S	77°11.865'W	88	nutrients
M137 - 728	16.05.17	02:23	MSS 28	12°13.754'S	77°29.714'W	170	
M137 - 729	16.05.17	03:15	CTD 48	12°15.099'S	77°29.606	182	nutrients
M137 - 730	16.05.17	04:43	MSS 29	12°20.13'S	77°21.76'W	181.6	
M137 - 731	16.05.17	05:33	CTD 49	12°21.36'S	77°21.68'W	191.6	nutrients
M137 - 732	16.05.17	07:15	MSS 30	12°26.06'S	77°12.95'W	170.1	
M137 - 733	16.05.17	07:55	CTD 50	12°26.82'S	77°12.93'W	178.6	nutrients
M137 - 734	16.05.17	13:20	MUC 23	12°37.787'S	77°21.352'W	512.6	
M137 - 735	16.05.17	14:23	MUC 24	12°38.143'S	77°20.740'W	489.1	
M137 - 736	16.05.17	16:21	ISP 08	12°27.243'S	77°29.243'W	400	
M137 - 737	16.05.17	18:38	CTD 51	12°27.243'S	77°29.243'W	400	
M137 - 738	16.05.17	19:45	TM CTD 77	12°27.24'S	77°29.24'W	397	
M137 - 739	16.05.17	21:52	BIGO-II-4	12°21.501'S	77°21.708'W	190	deployment
M137 - 740	16.05.17	23:00	MSS 31	12°18.832'S	77°19.159'W	154	
M137 - 741	17.05.17	01:07	CTD 52	12°20.235'S	77°19.902'W	172	nutrients
M137 - 742	17.05.17	02:44	MSS 32	12°32.482'S	77°21.570'W	409	
M137 - 743	17.05.17	03:45	CTD 53	12°33.892'S	77°21.584'W	418	nutrients
M137 - 744	17.05.17	05:39	MSS 33	12°26.25'S	77°29.39'W	384	
M137 - 745	17.05.17	06:22	CTD 54	12°26.97'S	77°29.58'W	404	nutrients
M137 - 746	17.05.17	08:12	MSS 34	12°19.07'S	77°35.97'W	422	
M137 - 747	17.05.17	09:11	CTD 55	12°19.56'S	77°36.07'W	493.5	nutrients
M137 - 748	17.05.17	13:04	MUC 25	12°21.582'S	77°21.763'W	195.7	
M137 - 749	17.05.17	15:00	cancelled				drifting nets
M137 - 750	17.05.17	16:00	ISP 09	12°22.59'S	77°26.15'W	262	
M137 - 751	17.05.17	19:00	MUC 26	12°23.999'S	77°24.277'W	244	
M137 - 752	17.05.17	19:58	CTD 56	12°22.597'S	77°26.157'W	261	
M137 - 753	17.05.17	21:12	RAP CST 09	12° 20.26' S	77° 21.73' W	182	
M137 - 754	17.05.17	23:00	BIGO-I-4	12°13.504'S	77°10.799'W	75	deployment
M137 - 755	18.05.17	13:21	BIGO-II-4	12°21.479'S	77°21.877'W	194	recovery
M137 - 756	18.05.17	14:34	MUC 27	12°23.249'S	77°24.269'W	242	
M137 - 757	18.05.17	17:00	ISP 10	12°31.25'S	77°34.88'W	734	
M137 - 758	18.05.17	20:36	TM CTD 78	12°31.34'S	77°35.05'W	750	
M137 - 759	18.05.17	21:31	CTD 57	12°31.384'S	77°35.196'W	764	
M137 - 760	18.05.17	22:13	MSS 35	12°31.567'S	77°35.126'W	789	
M137 - 761	18.05.17	23:48	CTD 58	12°31.373'S	77°35.045'W	756	nutrients
M137 - 762	19.05.17	01:27	MSS 36	12°28.167'S	77°32.104'W	478	
M137 - 763	19.05.17	02:29	CTD 59	12°29.899'S	77°32.867'W	547	nutrients

Station #	Date	Time (UTC)	Gear #	Latitude	Longitude	Depth (m)	Remarks
M137 - 764	19.05.17	04:25	MSS 37	12°23.53'S	77°25.57'W	266	
M137 - 765	19.05.17	05:38	CTD 60	12°24.81'S	77°26.10'W	298	nutrients
M137 - 766	19.05.17	06:48	MSS 38	12°22.21'S	77°23.66'W	297	
M137 - 767	19.05.17	07:37	CTD 61	12°23.02'S	77°23.89'W	232	
M137 - 768	19.05.17	09:12	CTD 62	12°18.72'S	77°17.73'W	144	
M137 - 769	19.05.17	09:30	MSS 39	12°18.92'S	77°17.67'W	144	cancelled. high swell
M137 - 770	19.05.17	13:13	BIGO-I-4	12°13.564'S	77°10.703'W	75	recovery
M137 - 771	19.05.17	14:40	MUC 27	12°16.731'S	77°14.947'W	127.6	
M137 - 772	19.05.17	16:04	MUC 28	12°21.573'S	77°21.738'W	195	
M137 - 773	19.05.17	16:35	MUC 29	12°24.540'S	77°21.633'W	195	
M137 - 774	19.05.17	17:00	MUC 30	12°21.55'S	77°21.60'W	194	
M137 - 775	19.05.17	17:57	MUC 31	12°23.286'S	77°24.276'W	243	
M137 - 776	19.05.17	19:10	MUC 32	12°24.898'S	77°26.293'W	303	
M137 - 777	19.05.17	22:13	BIGO-II-5	12°16.96'S	77°14.984'W	126.6	deployment
M137 - 778	19.05.17	22:37	MSS 40	12°16.66'S	77°15.008'W	130	
M137 - 779	19.05.17	23:58	CTD 63	12°16.737'S	77°14.938'W	128	nutrients
M137 - 780	20.05.17	01:02	MSS 41	12°14.39'S	77°12.40'W	92	
M137 - 781	20.05.17	02:41	CTD 64	12°15.087'S	77°12.866'W	106	nutrients
M137 - 782	20.05.17	04:33	MSS 42	12°13.068'S	77°10.482'W	68	
M137 - 783	20.05.17	04:59	CTD 65	12°13.51'S	77°10.78'W	75.8	nutrients
M137 - 784	20.05.17	06:44	MSS 43	12°17.83'S	77°17.36'W	137.7	
M137 - 785	20.05.17	07:45	CTD 66	12°18.68'S	77°17.77'W	143	nutrients
M137 - 786	20.05.17	10:07	RAP CST 10	12° 28.11' S	77° 29.15' W	409.9	
M137 - 787	20.05.17	13:04	MUC 33	12°14.80'S	77°12.70'W	103.4	
M137 - 788	20.05.17	15:50	MUC 34	12°27.195'S	77°29.296'W	412.6	
M137 - 789	20.05.17	20:38	ISP 11	12°32.875'S	77°34.769'W	824	
M137 - 790	20.05.17	21:13	CTD 67	12°33.158'S	77°34.651'W	838	
M137 - 791	20.05.17	23:43	BIGO-I-5	12°24.91'S	77°26.29'W	302	deployment
M137 - 792	21.05.17	01:50	TM CTD 79	12°30.99'S	77°34.57'W	750	
M137 - 793	21.05.17	04:37	MSS 44	12°17.115'S	77°30.346'W	225	
M137 - 794	21.05.17	05:43	CTD 68	12°18.57'S	77°30.18'W	253.4	nutrients
M137 - 795	21.05.17	07:11	MSS 45	12°22.38'S	77°23.90'W	222	
M137 - 796	21.05.17	08:01	CTD 69	12°23.23'S	77°24.08'W	234	nutrients
M137 - 797	21.05.17	09:50	CTD 70	12°31.01'S	77°17.35'W	284	nutrients
M137 - 798	21.05.17	10:24	MSS 46	12°31.14'S	77°17.37'W	285.9	
M137 - 799	21.05.17	13:17	BIGO-II-5	12°16.814'S	77°14.952'W	130	recovery
M137 - 800	21.05.17	16:42	MUC 35	12°38.153'S	77°20.728'W	503	no sediment
M137 - 801	21.05.17	17:45	MUC 36	12°38.142'S	77°20.415'W	496	
M137 - 802	21.05.17	20:00	ISP 12	12°34.81'S	77°40.33'W	980	
M137 - 803	21.05.17	23:44	TM CTD 80	12°34.81'S	77°40.33'W	972	
M137 - 804	22.05.17	00:46	CTD 71	12°34.992'S	77°40.395'W	982	
M137 - 805	22.05.17	01:43	MSS 47	12°35.108'S	77°40.455'W	991	
M137 - 806	22.05.17	02:59	CTD 72	12°34.911'S	77°40.318'W	977	nutrients

Station #	Date	Time (UTC)	Gear #	Latitude	Longitude	Depth (m)	Remarks
M137 - 807	22.05.17	04:22	MSS 48	12°36.64'S	77°43.76'W	1086	
M137 - 808	22.05.17	05:16	CTD 73	12°37.47'S	77°43.67'W	1150	nutrients
M137 - 809	22.05.17	07:27	CTD 74	12°32.43'S	77°37.88'W	921.5	nutrients
M137 - 810	22.05.17	09:00	MSS 49	12°28.03'S	77°31.54'W	496.6	
M137 - 811	22.05.17	09:54	CTD 75	12°28.70'S	77°31.67'W	508.1	nutrients
M137 - 812	22.05.17	13:14	BIGO-I-5	12°24.980'S	77°26.244'W	305	recovery
M137 - 813	22.05.17	14:28	MUC 37	12°23.294'S	77°24.271'W	242.2	
M137 - 814	22.05.17	17:00	ISP 13	12°34.91'S	77°40.35'W	980	
M137 - 815	22.05.17	20:08	CTD 76	12°34.910'S	77°40.350'W	966	
M137 - 816	22.05.17	21:09	RAP CST 11	12° 34.91' S	77° 40.27' W	966.4	
M137 - 817	23.05.17	00:55	BIGO-II-6	12°13.49'S	77°10.78'W	74.8	blind deployment
M137 - 818	23.05.17	02:21	MSS 50	12°20.409'W	77°04.093'W	101	
M137 - 819	23.05.17	03:30	CTD 77	12°21.254'S	77°03.820'W	106	nutrients
M137 - 820	23.05.17	05:17	MSS 51	12°14.25'S	77°12.23'W	92.2	
M137 - 821	23.05.17	06:14	CTD 78	12°14.99'S	77°12.77'W	103.2	nutrients
M137 - 822	23.05.17	07:41	CTD 79	12°08.19'S	77°18.33'W	109.2	nutrients
M137 - 823	23.05.17	08:17	MSS 52	12°08.20'S	77°18.32'W	109.5	
M137 - 824	23.05.17	11:08	TM CTD 81	12°21.50'S	77°21.71'W	193.2	
M137 - 825	23.05.17	13:08	MUC 38	12°21.51'S	77°21.72'W	193	2nd try successful
M137 - 826	23.05.17	14:41	MUC 39	12°24.903'S	77°26.280'W	301	
M137 - 827	23.05.17	15:16	MUC 40	12°24.903'S	77°26.256'W	302	
M137 - 828	23.05.17	17:11	Glider IFM03	12°39.03'S	77°28.86'W	893	recovery
M137 - 829	23.05.17	18:02	RPD CST 12	12°37.65'S	77°28.01'W	767.8	
M137 - 830	23.05.17	21:47	BIGO-I-6	12°13.544'S	77°10.678'W	75.4	blind deployment
M137 - 831	23.05.17	22:10	RPD CST 13	12°13.58'S	77°10.93'W	76	
M137 - 832	24.05.17	00:17	MSS 53	12°12.20'S	77°32.55'W	183	
M137 - 833	24.05.17	03:03	MSS 54	12°11.890'S	77°35.231'W	237	
M137 - 834	24.05.17	07:06	MSS 55	12°12.53'S	77°37.73'W	541.1	
M137 - 835	24.05.17	08:45	TM CTD 82	12°15.30'S	77°42.06'W	1234.5	
M137 - 836	24.05.17	13:16	BIGO-II-6	12°13.606'S	77°10.917'W	75	recovery
M137 - 837	24.05.17	13:00	ISP 14	12°13.608'S	77°10.96'W	76.7	
M137 - 838	24.05.17	17:06	MUC 41	12°13.473'S	77°10.855'W	75	
M137 - 839	24.05.17	17:55	MUC 42	12°13.475'S	77°10.846'W	75	
M137 - 840	24.05.17	19:35	MUC 43	12°18.695'S	77°17.786'W	144	
M137 - 841	24.05.17	20:35	MUC 44	12°17.011'S	77°14.704'W	130	
M137 - 842	24.05.17	21:46	CTD 80	12°13.600'S	77°10.912'W	75	
M137 - 843	24.05.17	22:24	MSS 56	12°13.605'S	77°10.922'W	69	
M137 - 844	24.05.17	23:55	CTD 81	12°14.377'S	77°11.203'W	85	
M137 - 845	25.05.17	01:22	MSS 57	12°25.959'S	77°12.056'W	163	
M137 - 846	25.05.17	02:36	CTD 82	12°27.316'S	77°12.941'W	182	nutrients
M137 - 847	25.05.17	04:06	MSS 58	12°20.498'S	77°20.596'W	176	
M137 - 848	25.05.17	05:11	CTD 83	12°21.25'S	77°21.39'W	188.5	nutrients
M137 - 849	25.05.17	07:00	MSS 59	12°14.25'S	77°29.11'W	171.6	

Station #	Date	Time (UTC)	Gear #	Latitude	Longitude	Depth (m)	Remarks
M137 - 850	25.05.17	07:39	CTD 84	12°14.68'S	77°29.41'W	174.6	nutrients
M137 - 851	25.05.17	08:10	RAP CST 14	12°14.94'S	77°28.86'W	175.3	
M137 - 852	25.05.17	09:35	MSS 60	12°13.346'S	77°11.323'W	77	
M137 - 853	25.05.17	10:31	CTD 85	12°13.94'S	77°11.66'W	83.6	nutrients
M137 - 854	25.05.17	13:17	BIGO-I-6	12°13.560'S	77°10.710'W	76	recovery
M137 - 855	25.05.17	14:12	SLM	12°13.52'S	77°10.79'S	76.3	recovery from M136
M137 - 856	25.05.17	16:25	MUC 45	12°23.316'S	77°24.280'W	244	
M137 - 857	25.05.17	18:04	POZ Lander	12°16.50'S	77°15.02'W	128.1	recovery from M136
M137 - 858	25.05.17	20:50	MUC 46	12°27.203	77°29.506'W	410	
M137 - 859	25.05.17	11:45	TM CTD 83	12°28.977'S	77°31.074'W	501	
M137 - 860	25.05.17	22:36	MSS 61	12°28.977'S	77°31.074'W	460	
M137 - 861	25.05.17	23:48	CTD 86	12°28.380'S	77°31.020'W	491	nutrients
M137 - 862	26.05.17	00:56	MSS 62	12°25.976'S	77°29.036'W	370	
M137 - 863	26.05.17	01:44	CTD 87	12°26.848'S	77°29.488'W	397	nutrients
M137 - 864	26.05.17	03:44	MSS 63	12°29.696'S	77°16.908'W	255	
M137 - 865	26.05.17	04:26	CTD 88	12°30.629'S	77°17.278'W	275	nutrients
M137 - 866	26.05.17	06:09	MSS 64	12°22.38'S	77°23.89'W	222.2	
M137 - 867	26.05.17	06:47	CTD 89	12°23.07'S	77°24.08'W	236.3	nutrients
M137 - 868	26.05.17	08:19	MSS 65	12°17.00'S	77°29.91'W	215.1	
M137 - 869	26.05.17	08:50	CTD 90	12°17.74'S	77°30.07'W	234.4	nutrients
M137 - 870	26.05.17	11:18	MUC 47	12°16.685'S	77°14.989'W	129.4	
M137 - 871	26.05.17	11:46	RAP CST 15	12° 16.73' S	77° 15.06' W	128.1	
M137 - 872	26.05.17	17:25	Glider IFM09	12°20.00'S	78°03.00'W	1965	deployment
M137 - 873	26.05.17	18:11	CTD 91	12°20.66'S	78°02.23'W	1937	nutrients
M137 - 874	26.05.17	19:27	TM CTD 84	12°20.78'S	78°01.88'W	1911	
M137 - 875	27.05.17	11:11	TM CTD 85	12°58.88'S	78°11.30'W	4990	
M137 - 876	27.05.17	16:14	CTD 92	12°58.90'S	78°11.33'W	5097	
M137 - 877	28.05.17	14:57	Glider IFM13	12°51.92'S	77°47.36'W	2251	recovery
M137 - 878	28.05.17	19:35	Glider IFM07	12°35.48'S	77°15.58'W	1021	rec/dpl

Abbreviations of the different gears/Measured parameters

Water column

CTD: (CTD Watersampling rosette): Physical properties. nutrients
TM CTD: (Trace Metal CTD water sampling rosette): Trace metals
Glider: Physical properties. turbulence. O_2. Nitrate
ISP: radiotracer and sulphur geochemistry
MSS: (Microstructure Sensor): Physical properties and turbulence
RAP CST: (Rapid Cast): Physical properties
Fish: (Device for the continuous sampling of surface waters)

Benthos

BIGO-I. BIGO-II: (Biogeochemical observatory. lander): Geochemistry. Microbiology. Foraminifera
MUC: (Multiple corer video-guided): Geochemistry. Microbiology. Foraminifera
SLM: (Satelite lander MOLAB): ADCP current measurements
POZ Lander: (Physical Oceanography Lander): ADCP current measurements

8 Data and Sample Storage and Availability

The data were collected within the Kiel Sonderforschungsbereich (SFB) 754. In Kiel a joint data management team of GEOMAR and Kiel University organizes and supervises data storage and publication by marine science projects in a web-based multi-user system. In a first phase data are only available to the project user groups. After a three year proprietary time the data management team will publish these data by dissemination to national and international data archives, i.e. the data will be submitted to PANGAEA no later than 2020. Digital object identifiers (DOIs) are automatically assigned to data sets archived in the PANGAEA Open Access library making them publically retrievable, citeable and reusable for the future. All metadata are immediately available publically via the following link pointing at the GEOMAR portal (https://portal.geomar.de/metadata/leg/show/341106). In addition, the portal provides a single downloadable KML formatted file (https://portal.geomar.de/metadata/leg/kmlexport/341106), which retrieves and combines up-to-date cruise (M137) related information, links to restricted data and to published data for visualization e.g. in GoogleEarth.
The following data sets will become available: hydrological data from Glider, CTD casts, moorings, small sized satellite lander, and microstructure CTD; water column nutrient data from CTD/water sampling rosette casts; trace elements, nutrients, DOP/DON, particles from Trace Metal CTD rosette casts, water column and sediment radiotracer data from in situ pump, CTD casts and MUC deployments, porewater geochemistry from MUC, GC and BIGO Lander; in situ flux measurements from BIGO Lander; microbiological data from MUC and BIGO Lander.

Table 8.1. Overview of data availability. For data storage and availability please see text above.

Data type	Contact person: Name, Institute, e-mail
Water column	
CTD, ADCP	M. Dengler, GEOMAR, mdengler@geomar.de
Microstructure CTD	M. Dengler, GEOMAR, mdengler@geomar.de
Glider, POZ Lander	M. Dengler, GEOMAR, mdengler@geomar.de
Nutrients (CTD Rosette)	S. Sommer, GEOMAR, ssommer@geomar.de
Nutrients (Trace Metal CTD)	M. Hopwood, GEOMAR, mhopwood@geomar.de
DOP/DON	J. Meyer, GEOMAR, jumeyer@geomar.de
Radiotracer (in situ pump)	B. Gasser, GEOMAR, b.gasser@iaea.org
Bacterial sulfate reduction	T. Treude, UCLA, ttreude@g.ucla.edu
Benthos	
Porewater geochemistry	A. Dale, GEOMAR, adale@geomar.de
Benthic fluxes/ in situ experiments	S. Sommer, GEOMAR, ssommer@geomar.de
Ex situ experiments	A. Dale, GEOMAR, adale@geomar.de
Foraminifera (incubations)	N. Glock, GEOMAR, nglock@geomar.de
Foram. (genomics, transcriptomics)	A.S. Roy, CAU, sroy@ifam.uni-kiel.de
Polyphosphate in sulfur bacteria	S. Langer, IOW, simon.langer@io-warnemuende.de
Sulfate reduction in sediments	T. Treude, UCLA, ttreude@g.ucla.edu

9 Acknowledgements

We thank Captain Rainer Hammacher his officers and the crew of RV METEOR for their excellent support. They created a very professional working environment and contributed a lot to the success of this cruise. The friendly atmosphere aboard is greatly acknowledged. We thank the Peruvian Ministerio De La Producción for its support and the allowance to conduct research in Peruvian waters and we very much would like to acknowledge the support of the German Ministry of Foreign Affairs.
We would also like to express our gratitude to the Leitstelle METEOR/MERIAN for its valuable support. The ship time of RV METEOR was provided by the Deutsche Forschungsgemeinschaft. The collaborative research centre 754 "Climate – Biogeochemistry Interactions in the Tropical Ocean" is funded by the German Research Council. DFG.

10 References

Aschar-Sobbi, R., Abramov, A.Y., Diao, C., Kargacin, M.E., French, R. J., Pavlov, E., 2008 High Sensitivity, Quantitative Measurements of Polyphosphate Using a New DAPI-Based Approach. J Fluoresc 18 (5), 859–866.

Bernhard, J. M., Casciotti, K. L., McIlvin, M. R., Beaudoin, D. J., Visscher, P. T., Edgcomb, V. P., 2012a. Potential importance of physiologically diverse benthic foraminifera in sedimentary nitrate storage and respiration, J. Geophys. Res., 117, G03002, doi:10.1029/2012JG001949.

Bohlen, L., Dale, A. W., Sommer, S., Mosch, T., Hensen, C., Noffke, A., Scholz, F., Wallmann, K., 2011. Benthic nitrogen cycling traversing the Peruvian oxygen minimum zone. Geochimica et Cosmochimica Acta 75, 6094-6111.

Brink, K.H., 1983. The near-surface dynamics of coastal upwelling. Progress in Oceanography, 12, 223-257.

Brock, J., Rhiel, E., Beutler, M., Salman, V., Schulz-Vogt, H. N., 2012. Unusual polyphosphate inclusions observed in marine Beggiatoa strain. Antonie Van Leeuwenhoek*, 101*(2), 347-357.

Buesseler, K. O., Benitez-Nelson, C. R., Moran, S. B., Burd, A. B., Charette, M. A., Cochran, J. K., Coppola, L., Fisher, N. S., Fowler, S. W., Gardner, W., Guo, L. D., Gustafsson, O., Lamborg, C., Masque, P., Miquel, J. C., Passow, U., Santschi, P. H., Savoye, N., Stewart, G., Trull, T., 2006. An assessment of particulate organic carbon to thorium-234 ratios in the ocean and their impact on the application of Th-234 as a POC flux proxy, Mar. Chem., 100, 213-233, 10.1016/j.marchem.2005.10.013.

Chaigneau, A., Dominguez, N., Eldin, G., Vasquez, L., Flores, R., Grados, C., Echevin, V., 2013. Near-coastal circulation in the Northern Humboldt Current System from shipboard ADCP data J. Geophys. Res. Oceans, 118, 5251-5266, doi: 10.1002/jgrc.20328

Dale, A.W., Sommer S., Lomnitz, U., Bourbonnais, A., Wallmann, K., 2016. Biological nitrate transport in sediments on the Peruvian margin mitigates benthic sulfide emissions and drives pelagic N loss during stagnation events. Deep. Res. I, 112, 123–136.

Dale, A.W., Graco, M., Wallmann, K., 2017. Strong and dynamic benthic-pelagic coupling and feedbacks in a coastal upwelling system (Peruvian shelf). Front. Mar. Sci. 4, 29.

Erdem, Z., Schönfeld, J., Glock, N., Dengler, M., Mosch, T., Sommer, S., Elger, J., Eisenhauer, A., 2016. Peruvian sediments as recorders of an evolving hiatus for the last 22 thousand years. Quaternary Science Reviews, 137, 1-14, doi:10.1016/j.quascirev.2016.01.029.

Glock, N., Roy, A., Romero, D., Wein, T., Weissenbach, J., Revsbech, N.P., Høgslund, S., Clemens, D., Sommer, S., Dagan, T., (accepted) Metabolic preference of nitrate over oxygen as an electron acceptor in Foraminifera from the Peruvian oxygen minimum zone. PNAS

Glock, N., Schönfeldt, J., Eisenhauer, A., Hensen, C., Mallon, J., Sommer, S., 2013. The role of benthic foraminifera in the benthic nitrogen cycle of the Peruvian oxygen minmum zone. Biogeosciences, 10, 4767-4783.

Glud, R.N., Thamdrup, B., Stahl, H., Wenzhöfer, F., Glud, A., Nomaki, H., Oguri, K., Revsbech, N.P., Kitazato, H., 2009. Nitrogen cycling in a deep ocean margin sediment (Sagami Bay, Japan), Limnol. Oceanogr., 54, 723–734.

Grasshoff, K., Ehrhardt, M., and Kremling, K.: Methods of Seawater Analysis, Wiley-VCH, Weinheim, 1999.

Gutiérrez, D., Enríquez, E., Purca, S., Quipúzcoa, L., Marquina, R., Flores, G., Graco, M., 2008. Oxygenation episodes on the continental shelf of central Peru: Remote forcing and benthic ecosystem response. *Prog. Oceanogr.* 79, 177–189.

Hales, B., D. Hebert, Marra, J., 2009, Turbulent supply of nutrients to phytoplankton at the New England shelf break front, *J. Geophys. Res.*, 114, C05010, doi:10.1029/2008JC005011

Heller, M.I., Lam, P.J., Moffett, J.W., Till, C.P., Lee, J.-M., Toner, B.M., Marcus M.A., 2017. Accumulation of Fe oxyhydroxides in the Peruvian oxygen deficient zone implies non-oxygen dependent Fe oxidation. Geochim. Cosmochim. Acta 211, 174–193.

Høgslund, S., Revsbech, N.P., Kuenen, J.G., Jørgensen, B.B., Gallardo, V.A., van de Vossenberg, J., et al., 2009. Physiology and behaviour of marine Thioploca. ISME J 3 (6), 647–657.

Ivanenkov V. N., Lyakhin Y., 1978. Determination of total alkalinity in seawater. In Methods of Hydrochemical Investigations in the Ocean (eds. O. K. Bordovsky and V. N. Ivanenkov). Nauka Publishing House, pp. 110–114.

Kalvelage, T., Lavik, G., Lam, P., Contreras, S., Arteaga, L., Löscher, C.R., Oschlies, A., Paulmier, A., Stramma, L., Kuypers, M.M., 2013. Nitrogen cycling driven by organic matter export in the South Pacific oxygen minimum zone. Nature Geoscience, 6, 228-234.

Lomnitz, U., Sommer, S., Dale, A.W., Löscher, C.R., Noffke, A., Wallmann, K., Hensen C., (2016) Benthic phosphorus cycling in the Peruvian oxygen minimum zone. Biogeosciences, 13, 1367-1386.

Martin, P., Van Mooy, B.A.S., 2012. Fluorometric Quantification of Polyphosphate in Environmental Plankton Samples: Extraction Protocols, Matrix Effects, and Nucleic Acid Interference. Applied and Environmental Microbiology, 79 (1), 273–281.

Mosch, T., Sommer, S., Dengler, M., Noffke, A., Bohlen, L., Pfannkuche, O., Liebetrau, V., Wallmann, K., 2012. Factors influencing the distribution of epibenthic megafauna across the Peruvian oxygen minimum zone, Deep-Sea Res. I, 68, 123–135.

Noffke, A., Hensen, C., Sommer, S., Scholz, F., Bohlen, L., Mosch, T., Gracco, M., Wallmann, K., 2012. Benthic iron and phosphorous fluxes across the Peruvian oxygen minimum zone. Limnology and Oceanography 57, 851-867.

Noffke, A., Sommer, S., Dale, A.W., Hall, P.O.J., Pfannkuche, O., 2016. Benthic fluxes in the Eastern Gotland Basin (Baltic Sea) with particular focus on microbial mat ecosystems. Marine Systems, 158, 1-12.

Pietri, A., Echevin, V., Testor, P., Chaigneau, A., Mortier, L., Grados, C., Albert, A., 2014. Impact of a coastal-trapped wave on the near-coastal circulation of the Peru upwelling system from glider data *J. Geophys. Res. Oceans, 119*, 2109-2120, doi: 10.1002/2013JC009270.

Piña-Ochoa, E., Høgslund, S., Geslin, E., Cedhagen, T., Revsbech, N. P., Nielsen, L. P., Schweizer, M., Jorissen, F., Rysgaard, S., Risgaard-Petersen, N., 2010a, Widespread occurence of nitrate storage and denitrification among Foraminifera and *Gromiida*, P. Natl. Acad. Sci. USA, 107, 1148–1153.

Piña-Ochoa, E., Koho, K. A., Geslin, E., Risgaard-Petersen, N., 2010b. Survival and life strategy of the foraminiferan *Globobulimina turgida* through nitrate storage and denitrification, Mar. Ecol.- Prog. Ser., 417, 39–49.

Rapp, I., Schlosser, C., Rusiecka, D., Gledhill, M., Achterberg, E.P., 2017. Automated preconcentration of Fe, Zn, Cu, Ni, Cd, Pb, Co, and Mn in seawater with analysis using high-resolution sector field inductively-coupled plasma mass spectrometry. Analytica Chimica Acta, 976, 1-13. DOI: 10.1016/j.aca.2017.05.008.

Rippeth, T. P., P. Wiles, M. R. Palmer, J. Sharples, Tweddle, J. 2009. The diapcynal nutrient flux and shear-induced diapcynal mixing in the seasonally stratified western Irish Sea. Cont. Shelf Res., 29(13), 1580–1587.

Risgaard-Petersen, N., Langezaal, A. M., Ingvardsen, S., Schmid, M. C., Jetten, M. S., Op den Camp, H. J. M., Derksen, J. W. M., Piña-Ochoa, E., Eriksson, S. P., Nielsen, L. P., Revsbech, N. P., Cedhagen, T., van der Zwaan, G. J., 2006. Evidence for complete denitrification in a benthic foraminifer, Nature, 443, 93–96, 2006.

Rutgers van der Loeff, M. M., Sarin, M. M., Baskaran, M., Benitez-Nelson, C. R., Buesseler, K. O., Charette, M. A., Dai, M., Gustafsson, O., Masque, P., Morris, P. J., Orlandini, K., Rodriguez y Baena, A. M., Savoye, N., Schmidt, S., Turnewitsch, R., Voge, I., Waples, J. T., 2006. A review of present techniques and methodological advances in analyzing Th- 234 in aquatic systems, Mar. Chem., 100, 190-212.

Schafstall, J., Dengler, M., Brandt, P., Bange, H., 2010. Tidal-induced mixing and diapycnal nutrient fluxes in the Mauritanian upwelling region J. Geophys. Res., 115, C10014, doi:10.1029/2009JC005940.

Scholz, F., Löscher, C.R., Fiskal, A., Sommer, S., Hensen, C., Lomnitz. U., Wuttig, K., Göttlicher, J., Kossel, E., Steininger, R., Canfield, D.E., 2016. Nitrate-dependent iron oxidation limits iron transport in anoxic ocean regions. Earth Planetary Science Letters, 454, 272-281.

Slomp, C.P., Malschaert, J.F.P., Van Raaphorst, W., 1998. The role of adsorption in sediment-water exchange of phosphate in North Sea continental margin sediments. Limnol. Oceanogr. 43, 832–846.

Sommer, S., Linke, P., Pfannkuche, O., Schleicher, T., Schneider v. Deimling.J., Reitz, A., Haeckel, M., Flögel, S., Hensen, C., 2009. Seabed methane emissions and the habitat of frenulate tubeworms on the Captain Arutyunov mud volcano (Gulf of Cadiz), Mar. Ecol. Prog. Ser., 382, 69–86, doi: 10.3354/meps07956.

Sommer, S., Gier, J., Treude, T., Lomnitz, U., Dengler, M., Cardich, J., Dale, A.W., 2016. Depeltion of oxygen, nitrate and nitrite in the Peruvian oxygen minimum zone cause an imbalance of benthic nitrogen fluxes. Deep-Sea Research I, 113-122.

Sommer, s., Clemens, D., Yücel, M., Pfannkuche, O., Hall, P.O.J., Almroth-Rosell, E., Schulz-Vogt, H.N., Dale, A.W., 2017. Major bottom water ventilation events do not significantly reduce basin-wide benthic N and P release in the Eastern Gotland Basin (Baltic Sea). Frontiers Marine Science, 4:18. Doi: 10.3389/fmars.2017.00018.